

Review

# Signal processing and calibration procedures for in situ diode-laser absorption spectroscopy

P.W. Werle<sup>a,b,\*</sup>, P. Mazzinghi<sup>a</sup>, F. D'Amato<sup>a</sup>, M. De Rosa<sup>a</sup>, K. Maurer<sup>b</sup>, F. Slemr<sup>c</sup>

<sup>a</sup> National Institute for Applied Optics, 50125 Florence, Italy

<sup>b</sup> Institute for Meteorology and Climate Research, 82467 Garmisch-Partenkirchen, Germany

<sup>c</sup> Max-Planck Institute for Chemistry, Atmospheric Chemistry Department, 55128 Mainz, Germany

Received 13 July 2003; received in revised form 7 October 2003; accepted 7 October 2003

## Abstract

Gas analyzers based on tunable diode-laser spectroscopy (TDLAS) provide high sensitivity, fast response and highly specific in situ measurements of several atmospheric trace gases simultaneously. Under optimum conditions even a shot noise limited performance can be obtained. For field applications outside the laboratory practical limitations are important. At ambient mixing ratios below a few parts-per-billion spectrometers become more and more sensitive towards noise, interference, drift effects and background changes associated with low level signals. It is the purpose of this review to address some of the problems which are encountered at these low levels and to describe a signal processing strategy for trace gas monitoring and a concept for in situ system calibration applicable for tunable diode-laser spectroscopy. To meet the requirement of quality assurance for field measurements and monitoring applications, procedures to check the linearity according to International Standard Organization regulations are described and some measurements of calibration functions are presented and discussed. © 2003 Elsevier B.V. All rights reserved.

**Keywords:** Diode laser spectroscopy; Gas analysis; Signal processing; Drift; Calibration function; Permeation devices

## 1. Introduction

Measurements of atmospheric trace gases impose high demands on analytical instrumentation. The great number of gaseous pollutants and their generally low and variable concentrations with large local differences pose challenging requirements to analytical techniques. Thus, sensitive, selective and mobile or even portable instruments with a large dynamic range are needed. Tunable diode-laser spectroscopy (TDLAS) is being frequently used for the measurement of trace gases [1–10] and especially during the last years many new applications have been reported. Most of them are based on indium phosphide [11–30], antimonide [31–33] and lead-salt diode-lasers [34–58] as well as quantum cascade lasers [59–72]. The applications cover the fields of fundamental spectroscopy, atmospheric chemistry, air monitoring applications and field campaigns, airborne systems for tropospheric and stratospheric research and industrial

monitoring and process control. Since the recent advances in semiconductor laser based gas monitors have been reviewed in a previous issue [9] and this paper focuses on post-detection signal processing and calibration issues, the TDLAS principles are only briefly summarized here.

In most tunable diode-laser spectrometers a single narrow laser line is scanned over an isolated absorption line of the target species (Fig. 1a–c). To achieve the highest selectivity, analysis is made at low pressure, where the absorption lines are not substantially broadened by pressure. This type of measurement has developed into a very sensitive and general technique for monitoring many atmospheric trace species. The main requirement is that the molecule should have an infrared line-spectrum which is resolvable at the Doppler limit, which in practice includes most molecules with up to five atoms together with some larger molecules. Because TDLAS operates at reduced pressure it is not restricted in wavelength to the atmospheric windows such as 3.4–5 and 8–13  $\mu\text{m}$  that are free from  $\text{H}_2\text{O}$  and  $\text{CO}_2$  [73]. Direct absorption measurements have to resolve small changes in a large signal. For typical linestrengths an ambient concentration of 1 ppbv (1 ppbv =  $10^{-9}$  volume mixing ratio) produces a

\* Corresponding author. Fax: +49-040-3603-029218.

E-mail address: [pwwerle@ino.it](mailto:pwwerle@ino.it) (P.W. Werle).

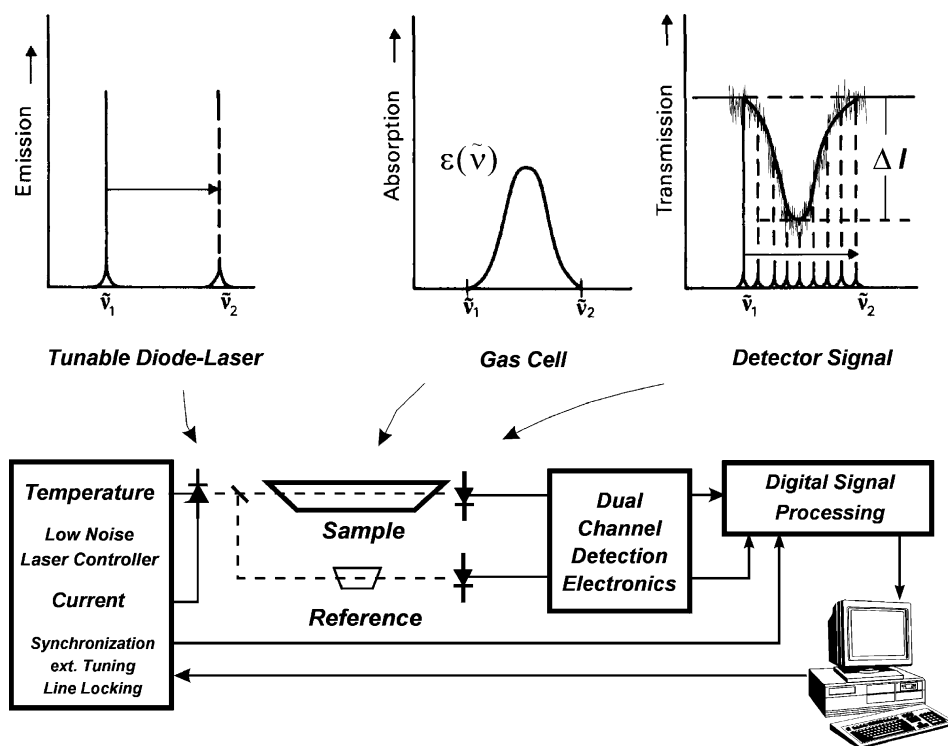


Fig. 1. Experimental set-up for TDLS: a single-mode emission of a temperature stabilized diode-laser is tuned by variation of the injection current over an absorption line of the gas under investigation in the absorption cell. The detector output signal of the transmitted intensity is amplified. Further signal processing leads to the final gas concentration.

line center absorption of only 1 part in  $10^7$  or lower over a 10 cm pathlength. Therefore, conventional absorption spectroscopy will not be able to measure such a small absorption. According to Beer's law one of the most important application of TDLS to atmospheric measurements has turned out to be their use in combination with a multi-pass cell with path lengths of 100 m or more. White [74] and Herriott and coworkers [75–77] cells achieve the long path by using mirrors to fold the optical path, giving typically 100 passes of a 1 m base-length cell. Additional modulation techniques like derivative spectroscopy using wavelength modulation in the kHz range or high frequency (MHz, GHz) modulation techniques based on single or two-tone modulation concepts are used to reduce the laser noise [9,78]. Modulation techniques produce a difference signal which is directly proportional to the species concentration (zero baseline technique) and allow the signal to be detected at a frequency at which the laser noise is significantly reduced. In these systems the diode-laser injection current is sinusoidally modulated as the laser wavelength is tuned through an absorption line. In general it is possible to monitor signals at all harmonics of the modulation frequency, although usually only the first and the second-harmonic signals are used. The normal mode of operating a TDLS system is to scan the laser center frequency through the absorption line repeatedly at about 0.1–1 kHz and use a computer-controlled signal averager to accumulate the signal with an amplitude proportional to the species concentration. Repetitive scanning over the line

gives increased confidence in the measurement because the characteristic feature of the measured species improves the signal-to-noise ratio (SNR) and unwanted spectral features due to interfering species or étalon fringes can easily be identified and sometimes can be reduced during the averaging process. With these techniques, detection limits of the order of 0.1 ppbv were achieved for many smaller molecules in air. In terms of optical density TDLAS instruments with a multipass absorption cell achieved detection limits on the order of  $10^{-6}$  with a 1 s integration time. The principal setup of a diode-laser spectrometer is shown in Fig. 1d. A prerequisite for a good signal-to-noise ratio is a low noise current- and temperature-controller for the laser. In many applications the atmospheric sample is pumped through a multipass cell, while a reference cell contains a constant high concentration of the target gas for line locking and diagnostic purposes. The signals from the sample and the reference detector are fed into a preamplifier. Then frequently a phase sensitive detection is applied and after that both channels are digitized and further processed by digital filters. This data post-processing also includes line locking, normalization and calibration procedures.

In the next section (Section 2), a concept for post-detection signal processing to deal with the influence of noise, jitter, drifts and fringes is presented. A strategy for the quantitative measurement of the system stability provides the basis for optimizing the measurement cycle. This in turn helps to obtain an improved system performance. The procedure for

the determination of the system performance according to the regulations of the International Standard Organization is summarized in Section 3. Procedures for spectrometer calibration based on standard gas mixtures and permeation based systems are described and finally some measurements of TDL calibration functions are discussed in Section 4.

## 2. Signal processing

### 2.1. Noise, jitter, drift and fringes

Trace gas measurements at ambient low levels are usually performed by measuring alternatively an ambient air spectrum and the spectrum of zero air, i.e. ideally ambient air devoid of the target substance, which often is referred to as a background spectrum. A prerequisite for quantitative measurements is a calibration spectrum recorded from a known gas mixture of known concentration in the sample cell. For monitoring of the laser amplitude and frequency fluctuations, a part of the laser beam is directed through a reference cell filled with a high concentration of the target gas (Fig. 1d) and a clean signal is generated, which is referred to as a reference spectrum.

The calculation of the gas concentration from the detector signal requires a clean structure and the signal-to-noise-ratio (SNR) is a convenient way to describe the “cleanliness” of a given signal level [79]. It is the signal voltage or power divided by the rms noise voltage (or power). Some examples of different SNRs are displayed in Fig. 2a–c. A spectrum obtained with a SNR of 100 or even more is a very clean pattern, with negligible noise. A SNR of 10 is a uncertain, but the pattern is still clear. At a SNR of 3, the signal is hardly recognizable, and at 1 the signal is almost lost. Ambient signals at low concentration levels generally have a poor SNR and, therefore, signal averaging is required prior to further signal processing. In addition, ambient, background and calibration signals used for data processing should have approximately the same signal-to-noise ratio. As noise, spikes, discrete and broadband interference, and drifts superimposed on the actual desired laser current manifest themselves as variations in the laser frequency, it is important to monitor these parameters. Typical tuning rates of lead-salt semiconductors used in spectroscopic instrumentation vary from several hundred MHz up to 2 GHz per mA. Therefore, a fluctuation in the laser current of only a few mA can cause laser wavelength fluctuations of some MHz. One approach to cope with these problems is the improvement of the laser current supply, e.g. by reducing the output bandwidth, but there are practical limits set by the scan frequency of the system. A different approach is to correct observed drifts on-line during the averaging process. The higher the number of channels per spectrum the higher is the precision which can be obtained by the correction algorithm. Discrete frequency interference superimposed on the laser current causes a jitter along the  $x$ -axis (wavelength). Co-averaging

of these spectra leads to a degraded system performance due to the broadening of the average spectrum. The implementation of a shift procedure eliminates or at least reduces the disturbances introduced by interfering signals. Even slow drifts can be eliminated with such an algorithm, and it is obvious that the quality of the shift mechanism depends on the number of channels in the ambient spectrum. Fig. 2d shows some experimental data, when the shifter software is implemented. Without the correction a significant jitter can be observed when several subsequent scans of spectra are plotted within the same graph, while the activated shifter reduces substantially a drift or jitter. This can be seen more clearly from the analysis in Fig. 2e, where calculated concentration values (upper trace) from a calibration source are plotted as a function of time. For this measurement a stable supply of calibration gas has been used for calibration first and then continuously as a sample. Therefore, the ratio of the measured signal ratio to the calibration signal should be 1, the ‘true’ concentration and consequently any deviation from 1 is not due to a concentration change, but refers to any other error in the system or analysis. This analysis revealed that without correction, the calculated concentration shows significantly lower values with much higher associated errors in the lower trace. The jitter correction is applied prior to co-averaging of the spectra and when it is active, a stable signal can be observed and the confidence range shown in the lower trace is at a reasonable low level and does not show changes with time.

While the laser is repetitively tuned across the absorption line under investigation, any wavelength drift has to be compensated. This process is usually called line-locking in TDLS. The most straight forward technique is to use a derivative signal from a reference cell filled with the target gas at a high concentration, which provides a clean signal. The number of the channel of the zero crossing of the first derivative as a characteristic feature can be used to determine a time dependent drift. If, for example, at the beginning of the measurements during a calibration the zero-crossing of the signal occurs at channel  $n$ , and after some time during a sample measurement has moved to  $n + \Delta$ , the quantity  $\Delta$  can be used in a feedback loop to bring back the laser to its initial center position by changing the injection current or the laser temperature. In contrast to the jitter correction described above, where the signal remains within an observation window, an actual feedback signal is applied to the laser controller here to keep the laser within this window. Fig. 2f shows a calibration signal in the center of the scan (dashed) and an ambient signal recorded some time later. The drift between calibration and ambient measurement is, in this case, about 10% of the laser scan. An investigation of the drift effect for an ambient signal with a signal amplitude of 50% of the calibration signal is shown in Fig. 2g. The dependence of the calculated concentration as a function of the drift is plotted for drifts up to 10% when the concentration is calculated by a linear regression. While the expected ‘true’ concentration is 0.5 for the 50% signal at zero drift

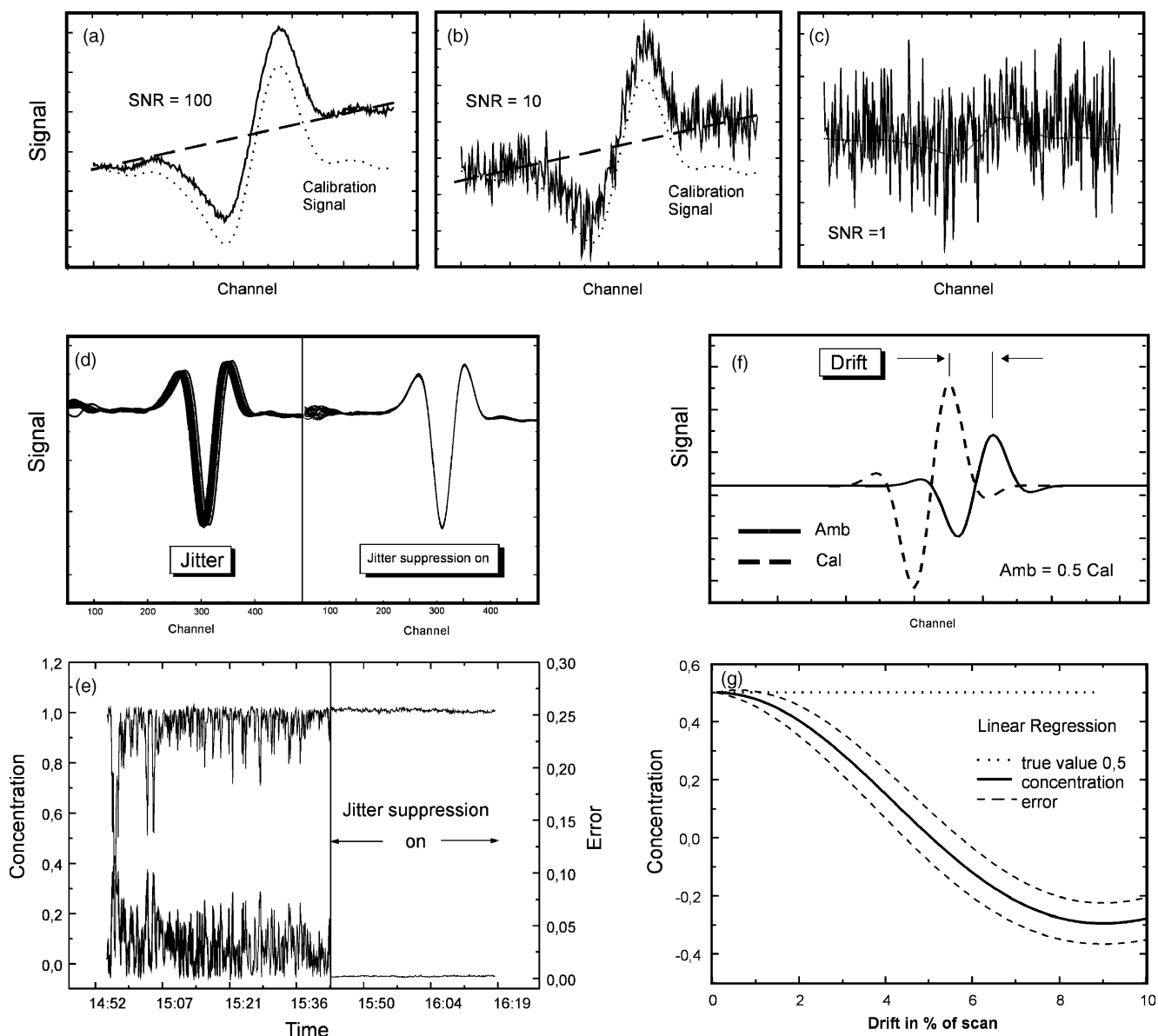


Fig. 2. (a) A signal-to-noise ratio (SNR) of 100 corresponds to a clean signal, (b) a SNR of 10 requires further signal averaging and (c) a SNR of 1 is noisy. (d) Fluctuations in the laser current translate into frequency jitter. (e) With active jitter suppression a significant increase in signal stability can be obtained. (f) Any drift between a calibration and ambient measurements can lead to (g) a significant underestimation of the 'true' concentration.

the simulation shows an underestimation at increasing drifts reaching even zero or negative concentrations.

Another frequently encountered limitation in diode-laser spectroscopy are time dependent background changes, which may originate from pressure broadened absorption lines from interfering atmospheric gases superimposed on the spectral feature of interest or from movement of optical fringes. Such fringes originate from optical resonators generated between optical elements in the laser path. Many resonators can be identified as potential sources, e.g. between the laser crystal and the detector crystal, any window or beamsplitter, or many others. Depending on their origin the superimposed fringe structure can be narrower, comparable or much broader than the spectral feature of the

target gas. For example, in the latter case we may observe a signal as shown in Fig. 2a with a time dependent slope generated from a broad moving fringe. In general fringe structure whose width is comparable to that from spectral features of interest present the most difficulties for accurate sample retrieval.

## 2.2. Adaptive signal processing

Signal processing concepts for fast scanning in situ diode-laser spectrometers are used to improve the SNR and to deal with time-dependent fringes. Therefore, they require three basic elements as shown in Fig. 3a. The first element is signal averaging to improve the signal-to-noise

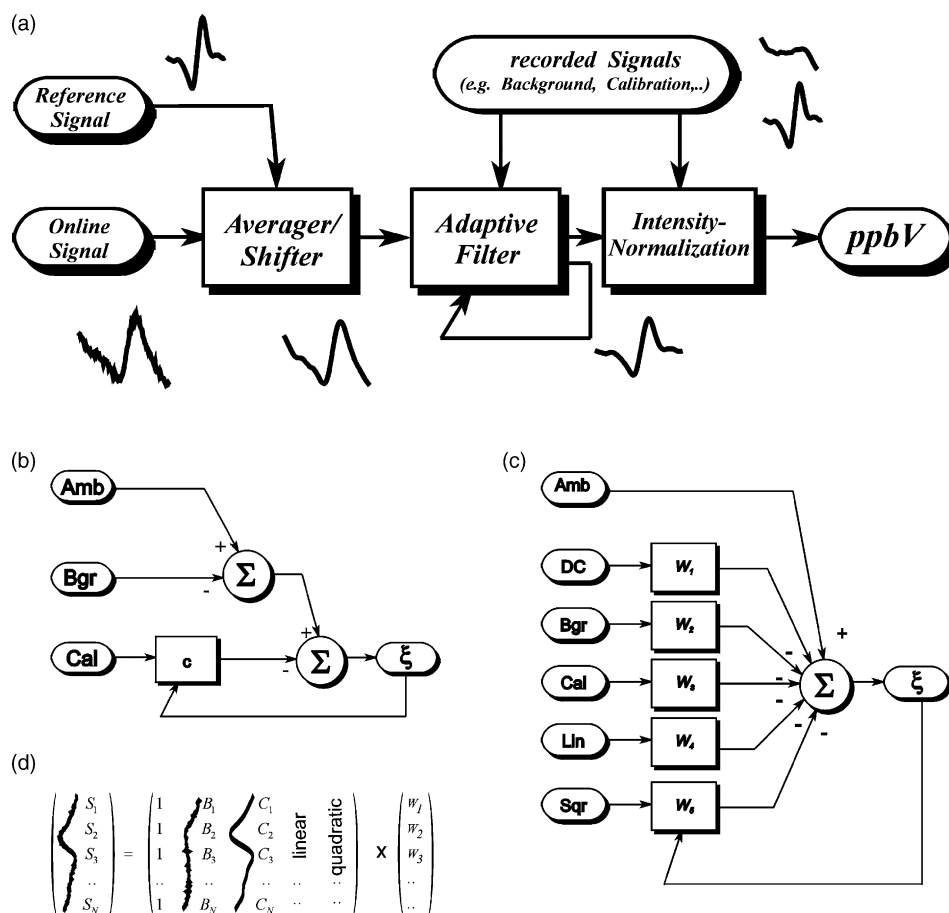


Fig. 3. (a) The main TDLS signal processing elements are SNR improvement and jitter correction, intensity normalization and an adaptive algorithm for the determination of the trace gas concentration under changing background conditions. (b) A linear regression scheme is the basic approach for signal processing. (c) The multiple linear regression scheme provides more flexibility to handle time time-dependent background changes and can be implemented in (d) matrix notation.

ratio and to smooth out the fast fluctuations in ambient spectra. The smoothed output of the signal averager is then fed into an adaptive digital filter. When a priori knowledge of the influence of background and fringes to the spectra is missing, adaptive algorithms are used, especially when superimposed signals are time dependent, nonlinear and have unknown dynamics with unknown disturbances acting upon them. Finally, a normalization process is applied to correct for amplitude variations and to determine the correct concentrations from ambient spectra. In addition a line locking algorithm should actively control the laser position.

The essential property of an adaptive system is its time-dependent, self-adjusting performance [79,80]. The need for such a performance may readily be seen by realizing that if the designer develops a system which he considers optimal, the implications are all possible input conditions are known. Specific criteria have to be defined to evaluate the system performance, which can be the amount of error between the output of the actual system and that of some selected model or ideal system. In sensitive spectrometers for trace gas analysis the complete range of input conditions may not be exactly known or the conditions may

change from time to time. In such circumstances, an adaptive system that continually seeks the optimum within an allowed class of possibilities (e.g. filters) would give superior performance compared with a system of fixed design. The generally available spectrometer data are the reference signal (Ref), the background signal (Bgr), a background corrected calibration signal (Cal) and the actual ambient signal (Amb). All spectra should contain  $n = 1, \dots, N$  data points. Additionally a vector containing information about the variances  $\sigma^2$  of the averaged signals may be available. The “desired” (synthetic) signal  $S$  should contain a fraction of the calibration signal Cal, the background and some possible other contributions, which have to be specified in detail. We can write the general performance criterion

$$\xi = \sum_{n=1}^N (\text{Amb}_n - S_n)^2, \quad (1)$$

and for the desired signal

$$S_n = f(\text{Bgr}_n, \text{Cal}_n, \dots) \quad (2)$$

Optimum conditions have been obtained when the desired signal matches the ambient signal. A frequently used approach for the function  $f$  is a linear combination of the arguments, e.g.

$$S_n = \text{Bgr}_n + c\text{Cal}_n \quad (3)$$

which can be applied in diode-laser spectroscopy, where a previously taken background (Bgr) spectrum is subtracted from the actual ambient spectrum (Amb) and then referenced to a calibration signal. This linear regression scheme (Fig. 3b) is based on a least mean square algorithm and, formally, we have to minimize the cost function  $\xi$

$$\xi = \sum_{n=1}^N \{(\text{Amb}_n - \text{Bgr}_n) - c\text{Cal}_n\}^2 \rightarrow \text{Min} \quad (4)$$

To determine the concentration  $c$ , we have to solve

$$\frac{\partial \xi}{\partial c} = 2 \sum_{n=1}^N \{-\text{Cal}_n \text{Amb}_n + \text{Cal}_n \text{Bgr}_n + c\text{Cal}_n^2\} = 0 \quad (5)$$

We can rewrite Eq. (5) as

$$\begin{aligned} -\gamma_{CA} + \gamma_{CB} + c\gamma_{CC} &= 0 \\ \gamma_{CA} &= \sum_{n=1}^N \text{Cal}_n \text{Amb}_n \\ \gamma_{CB} &= \sum_{n=1}^N \text{Cal}_n \text{Bgr}_n \\ \gamma_{CC} &= \sum_{n=1}^N \text{Cal}_n^2 \end{aligned} \quad (6)$$

and obtain for the concentration  $c$ .

$$c = \frac{\gamma_{CA} - \gamma_{CB}}{\gamma_{CC}} \quad (7)$$

This algorithm is sensitive to a slope in the background structure and extremely sensitive to even small drifts especially between calibration and ambient spectra (Fig. 2g). Depending on the direction of the slope, the signal is either under- or overestimated. Both effects can, under worst case conditions, lead to wrong concentration values without the possibility of a system operator or control software to identify such errors.

A more sophisticated approach is to apply a multiple linear regression (MLR) scheme shown in Fig. 3c. The multiple linear regression is an extension of the linear regression scheme and has more degrees of freedom for the fit process. While the previously discussed linear regression uses only information about the background and the structure of the calibration signal, the multiple linear regression scheme allows to add more parameters. A typical situation in diode-laser spectroscopy is the superposition of a more or less pronounced fringe structure to the ambient signal. If the free spectral range of the fringe is greater than the ambient signal, the fringe can manifest itself as a slope or another background structure with a curvature. A slowly moving fringe structure therefore generates a time dependent background structure which calls for adaptive signal processing in the previously discussed sense and we can write for the desired signal:

$$S_n = w_1 \text{Bgr}_n + w_2 \text{Cal}_n + w_3 \text{DC}_n + w_4 \text{Lin}_n + \dots + w_M \text{O}(n)_n \quad (8)$$

and for the performance function, which has to be minimized

$$\xi = \sum_{n=1}^N \{ \text{Amb}_n - (w_1 \text{Bgr}_n + w_2 \text{Cal}_n + w_3 \text{DC}_n + w_4 \text{Lin}_n + \dots + w_M \text{O}(n)_n) \}^2 \quad (9)$$

where the variable  $w_3$  contains then the magnitude of a DC offset. Background (Bgr), calibration (Cal), offset (DC), the linear slope (Lin) and all other vectors (spectra) with  $N$  elements appear as columns in the  $N \times M$ -matrix  $\phi$  (Fig. 3d) and the  $M$  coefficients  $w_\nu$ ,  $\nu = 1, \dots, M$  are the weights:

$$\text{Amb}_{N \times 1} = \phi_{N \times M} W_{M \times 1} \quad (10)$$

If we calculate the elements of the weight vector ( $w_1, \dots, w_M$ ) from the matrix  $\phi$  and the ambient signal, Amb, we obtain:

$$W = (\phi^T \phi)^{-1} \phi^T \text{Amb} \quad (11)$$

The value of  $w_2$  represents the ratio of the ambient signal to the calibration signal and thus can be used to determine the trace gas concentration. A prerequisite for these calculations is that  $\phi^T \times \phi$  can be inverted. The diagonal elements  $\text{cov}_{ii}$  in the covariance matrix  $\text{Cov} = (\phi^T \phi)^{-1}$  give the confidence range  $\Delta w$  for the  $M$  weights  $w$ .

While the multiple linear regression scheme is a multiple input filter with different signal sources, which uses the adaptive synthesis technique for the signal, other approaches are based on a single-input filter, which operates on sequential samples of the same signal [80]. A representative is the 'adaptive linear combiner' in the form of a single-input adaptive transversal filter. Some examples applying optimal filtering techniques to TDLS based on the Wiener and Kalman filter have been reported in the literature [81–85].

In spectroscopic measurements the detected signal is proportional to the trace gas concentration and also depends on the laser power. Intensity fluctuations of the laser or changes in the optical system alignment can generate a variation in the reported concentration data, which is not real. Therefore, an intensity normalization has to be applied to measured data. The laser intensity impinging upon the detector can be measured by coupling a certain amount of energy from the main beam using a beam splitter and monitor the laser power with a reference detector. A direct method is to monitor the average detector current, which is (after dark current subtraction) proportional to the number of photons incident upon the detector [81].

### 2.3. Characterization of system stability

The detection limits of a TDLS instrument should improve by averaging over a long time scale; but at optical densities of the order of  $10^{-6}$  the sensitivity is usually limited

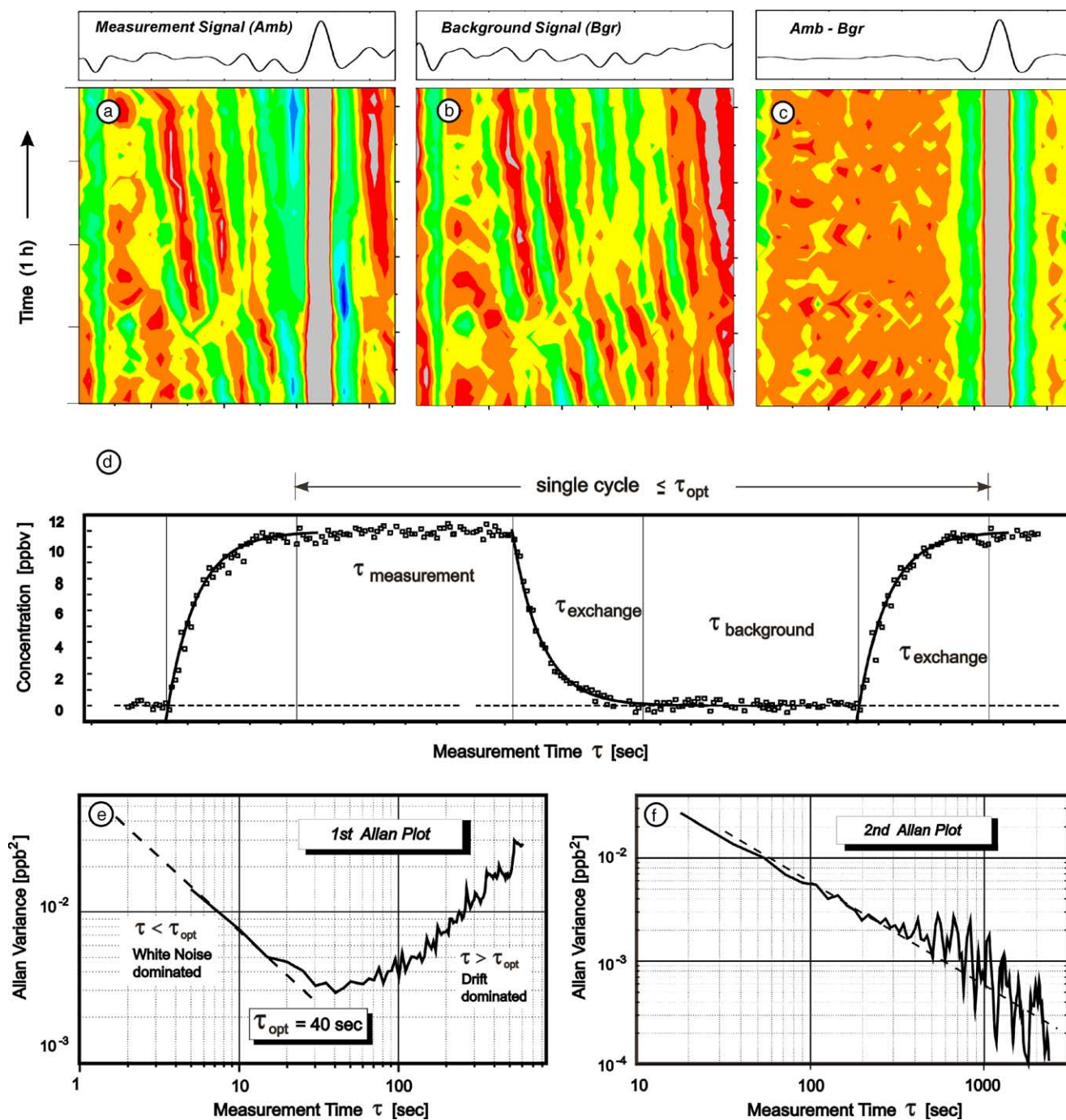


Fig. 4. The time dependence of (a) ambient measurement signals, (b) background signals and (c) the corrected signal is shown on a 1 h time scale. The stable traces in (a and c) are related to the fixed position of the molecular absorption. Background fluctuations can be efficiently suppressed by a scan by scan subtraction. (d) The optimum time for such a measurement cycle can be determined by an (e) Allan variance analysis. (f) After this optimization the Allan plot should follow the dashed line representing Gaussian ('white') noise.

by fringes due to unwanted étalons, which we can observe in Fig. 4a. In principle this limitation can be avoided by subtracting the background spectra as shown in Fig. 4b from the spectrum of ambient air in Fig. 4a. In these plots the temporal evolution of the spectral structure is shown with the horizontal axis corresponding to the spectral region (analysis window) and the vertical axis in each quadrant represent-

ing a time interval of about 1 h. The traces in Fig. 4b have been recorded when the measurement cell has been flushed with zero air. The stable vertical bar in Fig. 4a and c corresponds to the peak of the absorption line from the ambient signal, which shows only a slight variation in width. The other non stationary structures are generated by background drifts. As shown in Fig. 4c, improvement can be obtained

by measuring alternatively ambient and background spectra for the subtraction scheme. This subtraction-procedure inherently assumes that the instrument is stable during the time needed for the acquisition of both spectra, i.e. that the fringes do not move in the meantime. Practical measurements consist of a sequence of sample and background measurements. A typical measurement sequence is shown in Fig. 4d. After a period of ambient measurements the air in the sample cell has to be replaced by zero air to record background spectra. The exchange time for typical multipass cells varies from less than hundred milliseconds up to several seconds or even longer for sticky gases like ammonia or HNO<sub>3</sub>. Therefore, the exchange time can limit spectrometer performance due to a reduced duty cycle and drift effects.

The signal from a perfectly stable system could, in principle, be averaged infinitely. Infinite averaging should lead to extremely sensitive measurements, providing that limitations of the dynamic range of the system could be neglected. Unfortunately, real systems are stable only for a limited time, and it is obvious that every real unstable system will have an optimum averaging time given by the drifts in the system such as temperature drifts, moving fringes, changes in background spectra, etc. Consequently, the quality of the spectrometer is given by its stability described using the Allan variance [86]. The Allan variance as a function of the integration time,  $\tau$ , is the time average of the sample variance of two adjacent averages  $A_s(\tau)$  and  $A_{s+1}(\tau)$  of time series data:

$$\sigma_A^2(\tau) = \frac{1}{2m} \sum_{s=1}^m (A_{s+1}(\tau) - A_s(\tau))^2 \quad (12)$$

$$A_s(\tau) = \frac{1}{k} \sum_{l=1}^k x_{(s-1)k+l}, \quad s = 1, \dots, m$$

$\sigma_A^2(\tau)$  can be calculated by a computer and if plotted versus the integration time on a log–log plot gives the “Allan-plot” (Fig. 4e). The decreasing dashed line shows the theoretically expected behavior of a drift free system containing only white noise. Noise contributions encountered in most systems are frequency independent “white noise” and frequency dependent  $1/f$  and  $1/f^\alpha$  ( $\alpha > 1$ ) noise. The latter noise encompasses a noise at very low frequencies which can be considered as drift. The time domain stability,  $\sigma_A^2(\tau)$ , can be derived from the frequency domain stability and neglecting duty cycle effects for a first interpretation the Allan variance can be written in the following form as a time domain approximation [86]:

$$\sigma_A^2(\tau) = c_{\text{white noise}} \frac{1}{\tau} + c_{1/f} + \sum_{\alpha} c_{\text{drift},\alpha} \tau^\alpha \quad (13)$$

where  $\alpha$  characterizes the type of system drift. In the case of a linear drift,  $A_{s+1} - A_s = \text{const } \tau$ , we have  $\alpha = 2$ . This means that at short integration times,  $\tau$ , within the white noise dominated region, the Allan variance decreases (proportional to  $1/\tau$ ) with increasing integration time. As

the integration time increases, the Allan variance shifts from this region into a drift dominated region where it again starts to increase proportional to the measurement time. In the white noise dominated region the square root of the Allan variance is proportional to the detection limit and, therefore, can be used to predict the detection limit of a given system as a function of the integration time. The minimum in the Allan variance corresponds to the optimum integration time,  $\tau_{\text{opt}}$ , which is indicated in Fig. 4e. The optimum integration time is a characteristic property for a given instrument: it reflects the system stability (e.g. quality of line locking, drifts of fringes, changing background, etc.). The experimentally determined optimum integration time,  $\tau_{\text{opt}}$ , represents the time within which the sample and the background spectra have to be acquired:

$$\tau_{\text{opt}} \geq \tau_{\text{meas}}(\text{background}) + \tau_{\text{exchange}} + \tau_{\text{meas}}(\text{sample}) + \tau_{\text{exchange}} \quad (14)$$

where  $\tau_{\text{exchange}}$  is the time required for the removal of air from the absorption cell. For achieving the same signal-to-noise ratio the times for background and sample measurements should be set equal and therefore the actual optimum spectra measurement time is

$$\tau_{\text{meas}} = \frac{\tau_{\text{opt}} - 2\tau_{\text{exchange}}}{2} \quad (15)$$

If sample and background spectra are acquired subsequently and the integration times are chosen to be smaller or equal to  $\tau_{\text{meas}}$ , system drifts will not influence significantly the quality of the data. After this first drift correction the data can be stored again and analyzed in terms of the Allan variance again to find the maximum possible system integration time after the background has been removed. The Allan variance [86] can be used as a tool to characterize the overall stability of the spectrometer or its individual components (current controller, temperature controller, etc.) and to determine the optimum integration time. If the optimum integration time has been determined, the ambient and the corresponding background spectra must be measured within this time to make sure that no significant drift degrades the systems performance. This procedure significantly reduces drift effects. In principle, the observed drift effect should be eliminated but, practically, residual drifts will occur. It is important that the resulting data are again analyzed in terms of the Allan variance. The expected minimum resulting from this second Allan plot (Fig. 4f) gives an estimate for the ultimate sensitivity which can be achieved. However, integration times of 10 s of minutes may not be amenable for ambient measurements, particularly airborne measurements where one may experience large ambient concentration changes on time scales much faster than this.

### 3. Determination of the system performance

The application of modulation techniques does not allow a simple straightforward calculation of the measured

concentration from the measured signal. Additionally, for an accurate calculation of the concentration from the modulated absorption signal from first principles a precise knowledge of the line parameters (line strength, line width, pressure and temperature dependence) along with the modulation waveform and amplitude is necessary. Although many molecules have been carefully investigated, some data, e.g. in the HITRAN database [73] are known with an accuracy of only about 10–20%. Therefore, most instruments encompass a calibration system which offers the possibility to generate the necessary reference samples in the absorption cell as well as calibrate the entire inlet/sampling cell system. The usual way is to record spectra of zero-air or background, which is air devoid of the target substance, then a calibration gas at a known concentration level, and finally ambient air. The determination of the concentration of the target substance in ambient air is usually done by a regression analysis as it has been discussed in Section 2.2.

For an inter-comparison of system performance [87–90] it is necessary to give an international accepted description of the figure of merit of instruments, because most differences or discrepancies arise in the use of the associated terms like sensitivity, detection limit, determination limit, accuracy, and precision. Published detection limits differ quite a lot in the way they are obtained: for instance, it is done by analyzing the variation of the calibration gas or zero air over a certain time interval [86], by extrapolating to a signal-to-noise ratio of 1 at a certain electronic bandwidth or integration time [11,12], or by fitting the calibration spectrum to the difference of two background spectra [13], or sometimes the obtained values are multiplied by a factor of two or three to yield a specified statistical significance. All these methods assume a linear response of the instrument. Therefore, the linearity is checked by adding standards of varying concentrations [14,15]. The variety of methods makes it difficult to obtain a strictly rigorous comparison of different instruments. As the performance of diode laser systems is dynamic and each of the methods has unique advantages and disadvantages, ideally one should employ a variety of techniques. In field applications, one should employ these as frequently as possible.

Due to their high specificity, TDLAS instruments are used in air quality monitoring networks or in industrial process control. Consequently international accepted procedures have to be applied in order to determine the performance characteristics of the measurement method that is used. This paragraph follows the International Organization for Standardization ISO/DIS 9169 [91] regulation and related publications [92–95]: first of all, the steps of a measurement method (sampling, analysis, post-processing, calibration) have to be described. Thus, the test conditions must be representative of the intended operational measurements. All output signals evaluated throughout these tests must have been obtained after the measuring system has reached stable conditions.

The range of allowable averaging times is constrained by the requirements that the differences of subsequent output signals should be mutually statistically independent. By convention the minimum averaging time equals four times the response time (response time: time, when output signal reaches 90% after abruptly changing the value of the concentration). This has to be confirmed by an appropriate number of repetitions. After a instantaneous change of concentration the continuous mixing in the absorption cell shows an exponential behavior; a  $1/e$  – time of 1 s is equal to a response time of 2.3 s (Fig. 4d) and so the minimum averaging time is about 9 s. This time represents a 99.98% exchange of the gas.

A calibration experiment for the evaluation of performance characteristics consists of at least ten repeated measurements at a minimum of five different concentrations of the air sample. Throughout the remainder of this paper the following variables are used (see Fig. 5a):  $i$  varies from 1, ...,  $M$  and counts the sample number ( $M \geq 5$ ),  $j$  varies from 1, ...,  $N_i$  and counts the repeated measurements at one level ( $N_i \geq 10$ );  $N = \sum N_i$ ,  $c_i$  represents the concentration  $c$  in the  $i$ th sample, generated from reference material and  $x_{ij}$  is the  $j$ th output signal at  $c_i$ . The required tabulated data for different tests can be found in the literature [96–98]. A calibration experiment requires six steps. Beginning with the elimination of outliers we estimate the standard deviation  $s_i$  at  $c_i$  by

$$s_i^2 = \left\{ \sum_j x_{ij}^2 - \left( \sum_j x_{ij} \right)^2 / N_i \right\} / (N_i - 1) \quad (16)$$

Then the test characteristic TC can be derived with the group average  $\bar{x}_i$  at  $c_i$

$$TC = \left| \frac{x_{(i,j;\text{extr})} - \bar{x}_i}{s_i} \right|, \quad \bar{x}_i = \frac{1}{N_i} \sum_j x_{ij} \quad (17)$$

where  $x_{i,j;\text{extr}}$  is the output signal with the highest absolute distance from the mean output signal. The test characteristic TC has to be compared with tabulated values, and if it exceeds the critical value,  $x_{i,j;\text{extr}}$  has to be eliminated, (only if operational reasons can be found (but no more than 5% of data should be eliminated), e.g. for  $N_i = 20$  the critical value is 2.709. The dependence of  $s_i^2$  on  $c$  is modeled using:

$$\log \frac{\hat{s}^2}{s_0^2} = a_0 + a_1 \sqrt{\frac{c}{c_0}} + a_2 \left( \sqrt{\frac{c}{c_0}} \right)^2 \quad (18)$$

and consequently a smoothed variance function  $\hat{s}^2$  with weighting factor  $w$  at  $c$  is obtained:

$$\hat{s}^2(c) = s_0^2 \exp \left( a_0 + a_1 \sqrt{\frac{c}{c_0}} + a_2 \frac{c}{c_0} \right),$$

$$w(c) = \frac{s_0^2}{\hat{s}^2(c)} \quad (19)$$

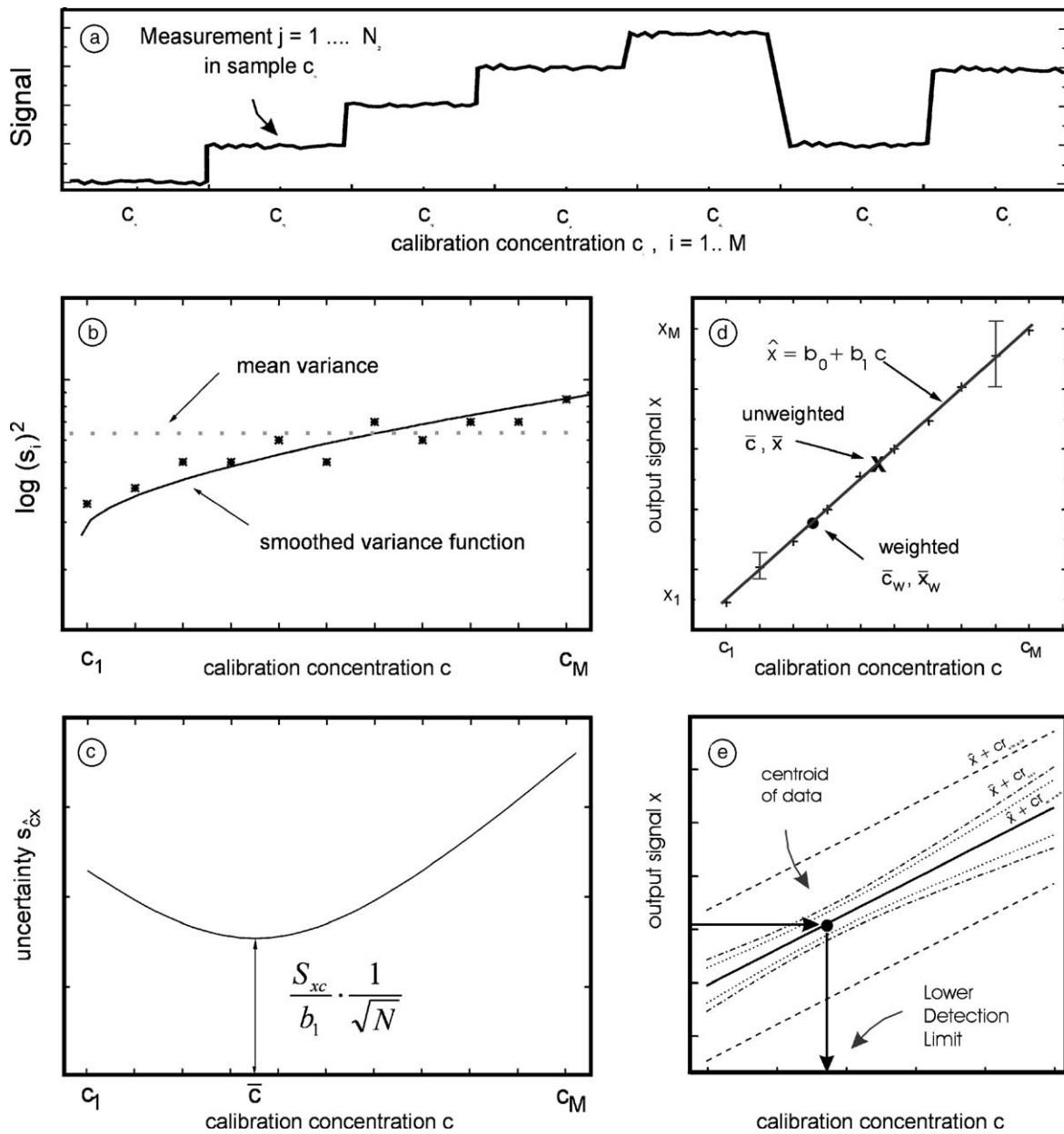


Fig. 5. (a) A set of calibration concentrations is used to record a calibration function. (b) Estimation of the variance function. (c) Estimation of the calibration function and position of the centroid in weighted and unweighted regression. (d) Uncertainty of the calibration function. (e) Different confidence limits derived from the calibration curve.

$s_0^2$  and  $c_0$  are normalization factors with magnitude 1, e.g. [ppbv],  $a_0, a_1, a_2$  are regression values [91]. This calculation of the variance function assumes a concentration-dependence of the variance (Fig. 5b). In a next step the calibration function is calculated. A linear calibration function can be estimated by

$$\hat{x} = b_0 + b_1 c \quad (20)$$

$$b_0 = \bar{x}_w - b_1 \bar{c}_w, \quad b_1 = \frac{\sum_i \sum_j w_i x_{ij} (c_i - \bar{c}_w)}{\sum_i N_i w_i (c_i - \bar{c}_w)^2} \quad (21)$$

with slope  $b_1$  and offset  $b_2$  and weighted average of calibration values  $c$  and weighted average of measured

values  $x$ :

$$\bar{c}_w = \frac{\sum_i N_i w_i c_i}{\sum_i N_i w_i}, \quad \bar{x}_w = \frac{\sum_i \sum_j w_i x_{ij}}{\sum_i N_i w_i} \quad (22)$$

The calculated line in Fig. 5e goes through the (weighted or unweighted) centroid of the data. An additional value  $s_{xc}$  can be calculated:

$$s_{xc} = \sqrt{\frac{\sum_i w_i \sum_j (x_{ij} - \hat{x}_i)^2}{\sum_i (N_i) - 2}} \quad (23)$$

$\hat{x}_i$  is the estimate of the output signal at  $c_i$ ,  $s_{xc}$  describes the scatter attributed to the estimation process outlined as

a whole. Without the weighting factors these formulas are identical to those in text books [96], where the following equations are used for calculation by computers. Using

$$\begin{aligned} Q_c &= \sum (c - \bar{c})^2 = \sum c^2 - \frac{(\sum c)^2}{N} \\ Q_x &= \sum (x - \bar{x})^2 = \sum x^2 - \frac{(\sum x)^2}{N} \\ Q_{cx} &= \sum (c - \bar{c})(x - \bar{x}) = \sum cx - \frac{\sum c \sum x}{N} \end{aligned} \quad (24)$$

one obtains:

$$b_1 = \frac{Q_{cx}}{Q_c}, \quad s_{xc} = \sqrt{\frac{Q_x - (Q_{cx})^2/Q_c}{N - 2}} \quad (25)$$

The hypothesis of linearity of the calibration function is tested using the statistic  $F$ -value which is defined as

$$F = \frac{\{\sum_i N_i w_i (\bar{x}_i - \hat{x}_i)^2\} / (M - 2)}{\{\sum_i \sum_j w_i (x_{ij} - \bar{x}_i)^2\} / \sum_i (N_i - 1)} \quad (26)$$

If  $F$  does not exceed the tabulated value  $F_{(M-2, N-M, 1-\alpha)}$  of the  $F$ -distribution [96] for the one-sided test for the specified significance level  $\alpha$ , non-linearity is negligible, e.g.  $F_{(3;45;0.95)} = 2.81$ . If  $F$  does exceed, then the subsequent performance characteristics can be calculated as an approximation provided the following inequality criterion holds:

$$\text{Max}_{i=1}^M \left\{ \frac{|\bar{x}_i - \hat{x}_i|}{2s_i} \right\} < 1 \quad (27)$$

or else the running procedure of determining performance characteristics must be aborted. (Tested is the ratio of ‘deviation of measured values from calculated values’ to ‘deviation of measured values from their group average’.)

The coefficients of the calibration function are estimates from a limited number of measurements. They will deviate from the true values which would be obtained with an unlimited set. The uncertainty of a deliberate measured value,  $c$ , under the calibration experiment, may be described by the estimate  $s_{\hat{c}_x}$  (Fig. 5c)

$$s_{\hat{c}_x} = s_{\hat{c}_x}(c) = \frac{s_{xc}}{b_1} \sqrt{\frac{1}{\sum_i N_i w_i} + \frac{(c - \bar{c}_w)^2}{\sum_i N_i w_i (c_i - \bar{c}_w)^2}} \quad (28)$$

The repeatability is calculated using

$$r = r(c) = t_{\nu; 1-\alpha/2} \frac{\sqrt{\hat{s}^2(c)}}{b_1} \sqrt{2} \quad (29)$$

where  $t$  is the two-sided Student- $t$ -factor, e.g.  $t = 2.262$  at  $\nu = 9$ ,  $\alpha = 0.05$  where  $\nu$  are the degrees of freedom:  $\nu = \min(N_i - 1)$ . As  $r$  refers to the difference between two single measurements the factor  $\sqrt{2}$  has to be included. The term reproducibility is used for inter-laboratory experiments (ISO 5725) [95]. The results are obtained with the same method on identical test material in different laboratories with different operators using different equipment.

The lower detection limit (LDL) at  $c = 0$  is defined as:

$$\text{LDL} = t_{\nu; 1-\alpha} \sqrt{s_r^2 + s_{\hat{c}_x}^2} \quad \text{with} \quad s_r = \frac{\sqrt{\hat{s}^2(0)}}{b_1} \quad (30)$$

where again the one-sided Student- $t$ -factor is used, e.g.  $t = 1.833$  at  $\nu = 9$ ,  $\alpha = 0.05$ .

The precision parameters depend strongly on the calculation of the variance function and the detection limit additionally on the uncertainty of the calibration function. The upper limit of measurement is approximated by the value of the air quality characteristic corresponding to the maximum measured value confirmed by the calibration process. It has to be noted that no extrapolations are allowed. ISO/DIS 5725/1 [95] defines a set of parameters which are related to precision parameters: accuracy is the closeness of agreement between test result and the accepted reference value. Trueness is the closeness of agreement between the average value obtained from a large series of test results and an accepted reference value. Bias is the difference between the expectation of the test results and an accepted reference value. Precision is the closeness of agreement between independent test results obtained under prescribed conditions. Furthermore, in ISO 9169 [91] the term sensitivity is used for the slope of the calibration function and in VDI 2449 [92–94] the determination limit is distinguished from the detection limit by another factor of 2. It is worth mentioning that in the literature different confidence ranges can be found [92,96,100]. Fig. 5e shows the confidence limit for the total regression line  $cr_{\text{tot}}$ , the confidence range for the expectation value  $\langle x \rangle$  at  $c$  and the prediction interval for a single measurement at  $c$ :

$$\begin{aligned} cr_{\text{tot}} &= \pm \sqrt{2F_{2, N-2; 1-\alpha/2}} s_{\hat{c}} \\ cr_{\text{mean}} &= \pm t_{N-2; \alpha} s_{\hat{c}} \\ cr_{\text{single}} &= \pm t_{N-2; \alpha} s_{\hat{c}} \end{aligned} \quad (31)$$

where

$$\begin{aligned} s_{\hat{c}} &= s_{xc} \sqrt{\frac{1}{N} + \frac{(c - \bar{c})^2}{Q_c}}, \\ s_{\hat{c}} &= s_{xc} \sqrt{1 + \frac{1}{N} + \frac{(c - \bar{c})^2}{Q_c}} \end{aligned} \quad (32)$$

In many text books the calculation of the correlation coefficient is recommended as a quality statement. But experiments will show that the correlation coefficient can be no more than a guide in making a decision [99] and additional criteria are needed. The linearity test described above is much more stringent.

## 4. Calibration procedures

### 4.1. Standard gas mixtures and permeation devices

Gas analyzers need to be calibrated and periodically checked to ensure system integrity and sensor accuracy. It

is important to install stationary sensors in monitoring networks in locations where the calibration can be performed easily. The intervals between calibration can be different from sensor to sensor. Generally, the minimum time interval between calibrations has to be determined for each sensor. However, it is good practice to carefully check the sensor during the first time after installation in order to observe how well the sensor is adapting to its environment and to investigate system stability and the required calibration intervals. Also, factors that were not accounted for in the design of the system might surface and can affect the sensor performance. If the sensor works properly for say 30 days, this provides a good degree of confidence about the installation. Any possible problems can be identified and corrected during this time. Experience indicates that a sensor surviving 30 days after the initial installation will have a good chance of good performance for the duration expected. Most problems – such as an inappropriate sensor location, interference from other gases, or the loss of sensitivity – will surface during this time. Afterwards, a maintenance schedule, including calibration intervals, should be established. The calibration procedure should be simple, straightforward, and easily executed by unskilled personnel. Calibration of routine and monitoring systems is simply a check, while research trace gas analyzers require a high degree of accuracy. For air quality and safety gas monitors, the calibration procedures need to be repeatable, economical, consistent, traceable and should be robust enough for field conditions. However, it is most important to keep the calibration methods standardized and easily traceable. Recent standardization deals with issues of gaseous ambient air measurement, indoor air pollution measurements and calibration procedures as a measure for quality assurance [101].

Calibration of a gas sensor involves two steps. First the “zero” must be determined and then the “span” must be set. There is no established standard that defines zero air. Many analytical procedures, including some specific analyzer procedures such as Environmental Protection Agency methods, use pure nitrogen or pure synthetic air to establish the zero point. The reason for this is that nitrogen and pure synthetic air in high pressure cylinders are readily available. As a result, it is believed that using bottled nitrogen or synthetic air is a good method to zero a sensor. Unfortunately, this is frequently not correct. Normal air contains traces of different gases besides nitrogen and oxygen and is usually humid. Therefore, it is much more realistic and practical to zero the sensor using the ambient air when it is considered to be unpolluted. For a specific target gas this reference point can be difficult to establish. Therefore, a good reference point can be in an area, where air is considered clean (e.g. in the mountains). This will give a more realistic representation of the zero point because it will be representative of the local ambient air condition. Compressed air has the advantage that it is easy to control and can be transported around in a cylinder, but may contain small concentrations of hydrocar-

bons, carbon monoxide, carbon dioxide, and possibly other interference gases. A solution to this is that the air can be filtered through activated charcoal to remove most of the unwanted gases and after this conditioning, compressed air can be used to calibrate most types of sensors. However, it is important to note that carbon monoxide is not removed by charcoal filters. It is therefore imperative to make sure that the CO concentration in the cylinder is the same as in the ambient air. Furthermore, a soda ash filter should be used as a scrubber to remove carbon dioxide. This is also a very good way to zero carbon dioxide sensors since placing a soda ash scrubber in-line with the sampling system will remove all carbon dioxide, thus providing an easily obtainable zero baseline.

The next step is span calibration, which can be easy or complicated and costly, depending on the gas type and concentration range. In principle, to achieve the best accuracy, a well defined mixture of the target gas in the ambient air is the best calibration gas. However, although the preparation of standard gas mixtures can be done, but it usually requires highly qualified personal. Therefore, most calibration gases are purchased from commercial suppliers. Premixed gas mixtures are the most common way to calibrate gas sensors. The mixture is compressed and stored under pressure in a gas cylinder. The cylinders are available in many sizes but most field calibrators employ smaller, lightweight cylinders. These small portable cylinders come in two different categories: a low-pressure and a high-pressure version. The low-pressure bottles are thin-walled, light-weight cylinders that are usually non-returnable and disposable. High-pressure cylinders are normally made of thick-walled aluminum which has a service pressure of 2000 psi and need to deliver the gas mixture through a regulator assembly [101]. This assembly consists of a pressure regulator, a pressure gauge, and an orifice flow restrictor. The orifice flow restrictor is a fitting with a hairline hole that allows a constant air flow at a given pressure difference. In operation, the high pressure from the bottle is reduced to a lower pressure of only a few psi, which provides a constant air flow through the orifice. Flow rates between 600 and 1000 cm<sup>3</sup> min<sup>-1</sup> are most common and can be adjusted using a pressure regulator. Many gases can be premixed with air and stored under pressure, but some gases can only be stored in an inert gas matrix, such as nitrogen. Some mixtures can only be stored in cylinders that are specially passivated or otherwise conditioned. Each type of mixture will have a different date of expiration. Detailed information about storage and shelf life can be obtained from the manufacturer. Generally, high vapor pressure gases with low reactivity, such as methane, carbon monoxide and carbon dioxide, can be mixed with air and stored under high pressure. Low vapor pressure gases, such as liquid hydrocarbon solvents, can only be mixed with air and stored under low pressure. Most highly reactive chemicals such as NO<sub>2</sub> are mixed with nitrogen. Gas standards in pressurized cylinders can be used as a gas source for subsequent dilution in a calibration gas system

or used directly when the concentration is within the operating range of the analyzer. Cylinders can be prepared in the laboratory or obtained commercially in various concentrations with or without certificate based on reference methods [102]. Such gas standards should be re-standardized against the reference method at a minimum of once every six months. The estimated volume of a pressurized gas in a cylinder is the total pressure ( $P$ ) divided by the atmospheric pressure ( $P_a$ ) multiplied by the volume,  $V$ , of the cylinder:

$$V_{\text{mix}} = V \left( \frac{P}{P_a} \right) \quad (33)$$

For example, a given lecture bottle has a 440 cm<sup>3</sup> volume ( $V$ ). Assume the bottle has a 1200 psi pressure. The estimated volume of the premixed gas at atmospheric pressure is: (440 cm<sup>3</sup>)(1200/14.7) = 35,918 cm<sup>3</sup>. If the flow rate of the calibration gas is 1000 cm<sup>3</sup> min<sup>-1</sup> and it takes approximately 1 min per sensor to calibrate, a single cylinder can be used to calibrate approximately 30 times.

Polar compounds, such as HNO<sub>3</sub>, NH<sub>3</sub>, alcohols and aldehydes, usually stick to surfaces and consequently, these mixtures are not stable when pressurized. For these compounds, permeation based systems are frequently used to calibrate gas analyzers [103–109]. Permeation devices are small, inert capsules containing a pure chemical compound in a two phase equilibrium between its gas phase and its liquid or solid phase (Fig. 6a). At a constant temperature, the device emits the compound through its permeable portion at a constant rate. Devices are typically inserted into a car-

rier flow to generate test atmospheres for calibrating gas analyzer systems. The tubular device is a sealed permeable cylinder containing the desired permeant gas and is the most widely used of the various permeation devices. The target compound permeates through the wall of the Teflon tube for the entire length between the impermeable plugs. A wide range of rates can be achieved by varying the length and thickness of the tube, with typical rates ranging from 5 to 50,000 ng min<sup>-1</sup>. Tubular permeation devices with active lengths (the length of the permeable section) ranging from 0.5 to 20 cm are available. Coupling of a standard tubular device to an impermeable stainless steel reservoir offers a range of permeation rates corresponding to a tubular device, but with up to ten times enhanced lifetime. Wafer devices have only a small permeable window, so permeation rates are typically lower than rates for tubular devices by an order of magnitude. Since permeation occurs only through the polymeric wafer, the permeation rate is controlled by varying the wafer material, the thickness of the wafer, the diameter of the permeation opening and the length of the permeable section. Gases whose high vapor pressure at normal permeation temperatures prevent their containment in a tubular device can be contained in a wafer device. Wafer devices are available in different types matching the calibrators made by various manufacturers. A permeation device, based on the diffusion of a gas through a semi-permeable membrane, can also be used as a gas source in a calibration gas system. The diffusion rate is a function of temperature and therefore constant temperature must be maintained

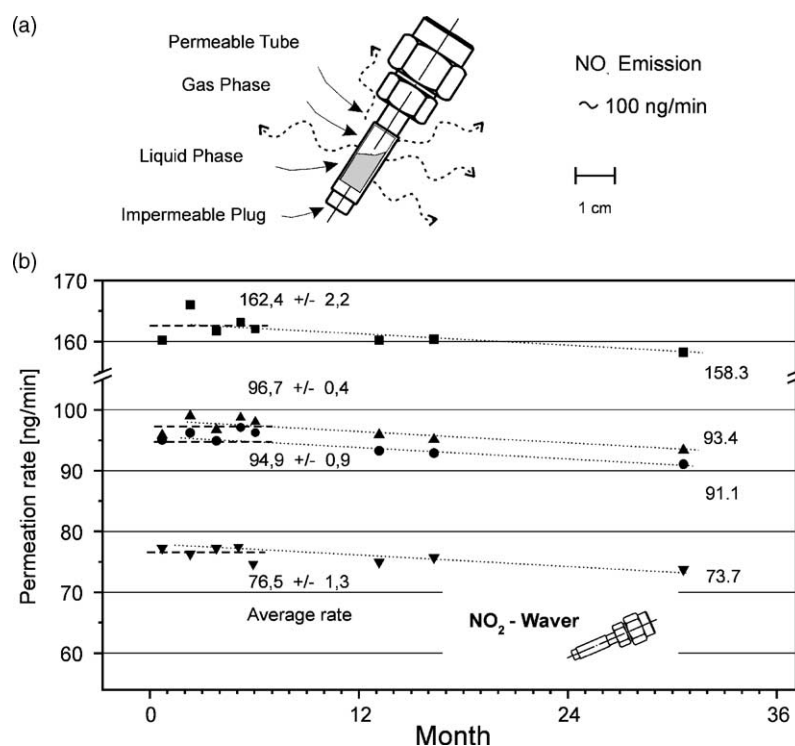


Fig. 6. (a) Schematic drawing of a permeation device for a typical emission of 100 ng NO<sub>2</sub> min<sup>-1</sup>. (b) Measurement of the NO<sub>2</sub> permeation rate during 3 years by periodical weighings of the tubes on a precision microbalance.

throughout the calibration. Certified permeation devices are usually standardized gravimetrically or against the accepted reference method at a minimum of once every six months. Precautions to be taken with permeation devices include: (i) storage of the device in a dry nitrogen atmosphere, preferably between 20 and 25 °C, (ii) use of a dry, analyte-free carrier gas and (iii) allowance of a minimum of 24 h for a permeation device to establish temperature equilibrium before use. The permeation rate of a wafer has to be gravimetrically determined by periodically weighing as indicated in Fig. 6b. However, the accuracy should be checked by other techniques, as can cite many examples where the additional gases permeating through the membrane will give rise to systematic calibration errors. The carbonyl sulfide permeation studies by Fried et al. [110] is one such example. The used of a calibrated microbalance gives an imprecision of 50 µg, leading to a precision of about 1 ng min<sup>-1</sup> within a 6 week interval. For all wafers the first measurement showed a significant higher value due to the wall saturation effects at the time of installation. Two wafers show a higher fluctuation than expected on the basis of gravimetric calibration; one reason seems to be the instability of the temperature control, because fluctuations of less than 1% of the emission rate are expected at a temperature stability of 0.1 K. As a rule of thumb each 1 °C increase in temperature increases the permeation rate by 10%. For a precise calculation the following equation can be used:

$$\log(Q_1) = \log(Q_0) + \alpha(T_1 - T_0) \quad (34)$$

where  $Q_0$  is the permeation rate at  $T_0$  (°C),  $Q_1$  the new rate at  $T_1$  (°C) and  $\alpha$  the temperature coefficient. As an estimate one may use  $\alpha = 0.030$  for high emission tubes and  $\alpha = 0.034$  for standard emission tubes. However, these values are not universal for every gas since they will not only depend upon the permeating material but also on the gas itself. Concentrations are expressed in mass per unit volume and parts per unit volume. Since the volume of gas varies with the temperature and pressure, standard conditions must be used in the computation and comparison of gases. Reference conditions are defined as 25 °C or sometimes 0 °C and 760 mmHg (1013 mbar). However, it does not matter what reference conditions are used as long as one uses the same conditions for the flow determination into which the permeating gas is mixed. The concentration of a calibration gas generated by a permeation tube in a dynamic carrier flow is calculated using the following equation:

$$c = \frac{Q}{F_c} \left( \frac{24.46}{m} \right) \quad (35)$$

where  $c$  is the concentration in ppm by volume,  $Q$  the permeation rate in ng min<sup>-1</sup>,  $m$  the molecular weight of the gas,  $F_c$  the flow of the calibration mixture in cm<sup>3</sup> min<sup>-1</sup>. The constant 24.46 is the molar volume at the reference conditions. To calculate parts per million concentration when using a pressurized gas standard for dilution the following

equation

$$c = \frac{F_c c}{F_0 + F_c} \quad (36)$$

is applied, where  $F_0$  is diluent air flow in cm<sup>3</sup> min<sup>-1</sup>,  $F_c$  calibration gas flow in cm<sup>3</sup> min<sup>-1</sup> and  $c$  concentration of the calibration gas in ppm. All parameters have to be corrected to the reference conditions according to

$$F_c = F_m \left( \frac{p}{760} \right) \left( \frac{298}{t + 273} \right) \quad (37)$$

where  $t$  is temperature in °C,  $F_m$  the measured flow rate and  $F_c$  the flow rate at reference conditions.

#### 4.2. Dynamic calibration

A dynamic calibration is a performance test of the entire analyzer system under simulated operating conditions. The system includes the analyzer, recorder and/or data transmission system, and the sampling system with its sample lines and sample filters. A first step for a dynamic calibration is to sample a zero air to establish an analyzer zero response (baseline). In a next step sample test-gas mixtures of known concentration from a calibration gas system are used to establish a response. A test-gas mixture with concentration approximately equal to mid-scale of the analyzer range should be used. The final analyzer response is obtained by subtracting the zero response (baseline) from the response to the test gas. The analyzer should be adjusted to make its response conform to the known test-gas concentration. After adjustments are made, it is necessary to repeat the sampling process to reestablish both the zero and analyzer response. Linearity and low level response are determined by varying the ratios of diluent air to calibration gas to provide test gas concentrations throughout the entire range of the analyzer. Zero air is used to establish a baseline point of reference and as a diluent in preparation of test gas mixtures. This air must be free of any substances which can alter the test gas mixtures or can affect the analyzer response or the reference method. A typical dynamic dilution system for the production of sub-ppb concentrations of reactive species has been described for example by Goldan et al. [111].

A calibration system for TDLS field applications requires a source of diluent air, a source of calibration gas, a mixing chamber and a delivery manifold from which analyzers and reference sampling trains can sample the test gas. The test gas is prepared by thoroughly mixing the calibration gas and diluent air in various known proportions. The calibration gas can be obtained from either from a set of permeation devices or from a pressurized cylinder containing a suitable concentration of the calibration gas. The calibration gas system should be positioned as close to the analyzer and reference sampling apparatus as is practical to minimize losses in the tubing. Sample lines, flow metering devices, mixing chambers, all other parts of the calibration system, as well as the analyzer system should be made of materials which will not

affect the test gas concentration. All components used in the calibration procedure should be allowed sufficient time to stabilize before reference samples are taken and before analyzer response is determined. Calibration records shall be maintained containing the information necessary to determine test gas concentrations and to determine the percent deviation of an analyzer's response to known test-gas concentrations. In airborne systems one has to contend with a variable ambient pressure into which the permeation standard is added. As a result, one must keep the permeation tube at constant pressure, using for example a pressure controller upstream of the permeation chamber and a glass capillary downstream, to avoid large instantaneous wall conditioning effects of the permeation device. The study by Fried et al. [112] is one such example of this behavior.

In order to provide the necessary air samples in the absorption cell, the calibration system in Fig. 7 shows a four chamber oven for permeation devices (operating temperature 20–40 °C, stability <0.1 K), a mixing chamber, the valves and flow controllers for gas flow handling, and a commercial closed loop pressure control unit for a White cell. The system can be operated in manual mode as well as under remote control of the host computer. Fig. 7 shows the gas flow of the system, when a special calibration cycle is selected.

In this configuration flow controller FC A provides up to  $11 \text{ min}^{-1}$  of the carrier gas ( $X1 + X3$ ) for the permeation oven chamber 1A and 2A. Oven 1B and 2B are supported by the main line and the flow  $X2 + X4$  is controlled by the capillary (flow is about  $20 \text{ ml min}^{-1}$ ) in front of each chamber and goes to the exhaust. By adjusting the set point of FC A higher than the sum of all four capillaries, always the same amount of gas – independent of the number of permeation chambers selected – flows into the mixing chamber, where a second dilution by the zero air flow controller FC E takes place (up to  $20 \text{ l min}^{-1}$ ). Mixing is an essential feature of any process for preparing a standard gas mixture. Great care must be exercised with flow systems, because laminar flow and stratification may lead to imperfect mixing. At flow rates of about  $50 \text{ l min}^{-1}$  mixing through a *t*-connection can be satisfactory, but usually mixing chambers are inserted in dynamical systems. However, two convenient methods for ensuring mixing are to allow two flows to impinge on each other at right angles or to let the major component flow at high velocity past the tip of a jet from which the minor constituent emerges, both flows being in the same direction. With the two valves following the mixing chamber it is possible to provide the gas (ambient/sample, background, calibration) for the absorption cell, and additionally, to add

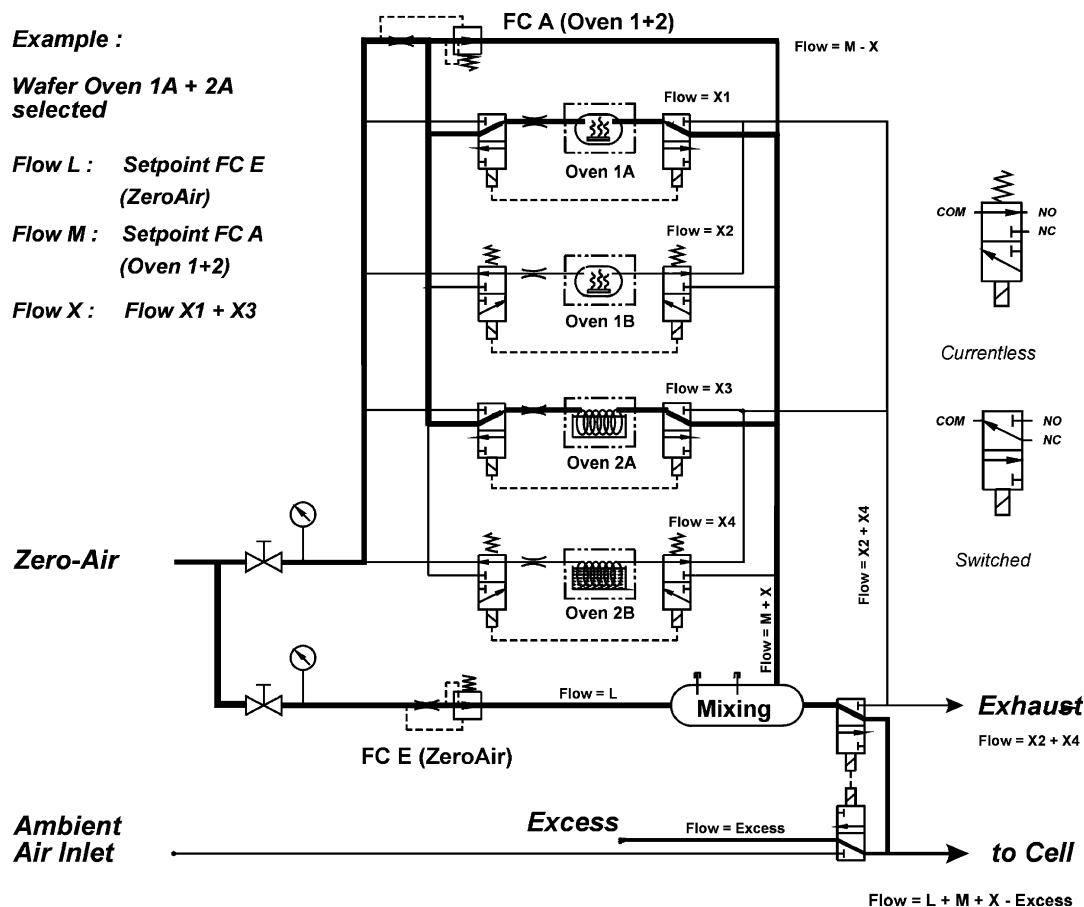


Fig. 7. A permeation based calibration system with two ovens (1/2) for independent temperature adjustments with two chambers (A and B) each. In this example, the flow through ovens 1A/2A is diluted with zero air in the mixing chamber and then directed into the measurement cell.

calibration gas to the sample gas flow. The mixing chamber has additional input ports for other calibration gas sources (e.g. compressed gas mixtures or another four chamber permeation oven). Sometimes it is necessary to add another dilution stage before the mixing chamber, in order to get the lower mixing ratio of the calibration gas. Consequently the system is designed (not shown in the picture) to dump a fraction of the first stage flow of FC A before it enters the mixing chamber. The design is similar to the system of Fried et al. [89]. A needle valve at the inlet of the absorption cell restricts the amount of gas in such a way that an excess flow is guaranteed. This system fulfills the requirements of the ISO regulations even for a multi-component spectrometer.

#### 4.3. Determination of a calibration function

Many applications in atmospheric research, medical diagnostics or industrial process control use compressed gas mixtures either as agents or as secondary reference standards for routine calibration of instruments. Therefore, exact knowledge of the quality of these gases is required, not only with respect to accuracy and precision of the specified concentration level of the components of interest, but also with respect to purity when considering gaseous contaminants. Since TDLS in the mid-infrared spectral region operates with high selectivity and sensitivity, this technique was chosen to control the quality of some selected pressurized gas mixtures at a concentration of the sensitive component specified to be below 200 ppbv. A description of the spectrometer – designed for ambient air measurements – can be found in [86]. For a sensitive and selective detection of NO<sub>2</sub>, a lead-salt diode-laser has been tuned to a strong absorption line at 1604.16 cm<sup>-1</sup> at an optical pathlength of 30 m in the multipass cell. The cell pressure is kept constant with an active pressure control loop typically at 50 mbar. The calibration of the spectrometer is done using the setup shown in Fig. 8 with the gas flow from the ambient inlet through the

optical multipass cell. The calibration system described in the previous section provides variable concentration levels in the range 3–40 ppbv NO<sub>2</sub> together with zero air and allows calibration with premixed calibration gas and additional dilution in the range 20–260 ppbv. All flow controllers were calibrated by two mercury sealed piston cylinders (Brooks Vol-U-Meter) in the range 1 ml min<sup>-1</sup> up to 15 l min<sup>-1</sup> with an accuracy of 0.1%. All flow values have been determined for standard conditions in temperature and pressure (STP). For the calculation of the concentration of the gas of interest three different spectra have to be recorded: background, calibration and sample. After subtraction of the background spectrum from the calibration and sample spectra the sample concentration is determined by a multi-linear regression analysis. For an improved sensitivity, jitter suppression, signal averaging and a normalization have been applied.

The calibration function for NO<sub>2</sub> measurements has been recorded after the flow controller calibration. A constant flow of zero air was used and the calibration signal generated by four permeation devices corresponds to 37 ppbv NO<sub>2</sub>. 50 measurement values for each concentration level were recorded and calibration and background measurements were repeated before changing to the next concentration. At the end of the measurement cycle also the sum of the two low permeation rate wafers were added to the dilution flow in order to obtain a value at a small concentration (1.3 ppbv). In this manner the calibration function was recorded using 18 concentration levels, but due to two nearly identical wafers only 13 widely spaced concentration levels can be seen in Fig. 9a. The corresponding calibration function is shown in Fig. 9b. A single concentration level was found to be an outlier due to incorrect operation during calibration, where a sudden change in the background structure occurred resulting in an offset of about 3 ppbv. This concentration level has been removed from the data set for further analysis. The hypothesis of linearity has to be rejected when the number of values per concentration level exceeds

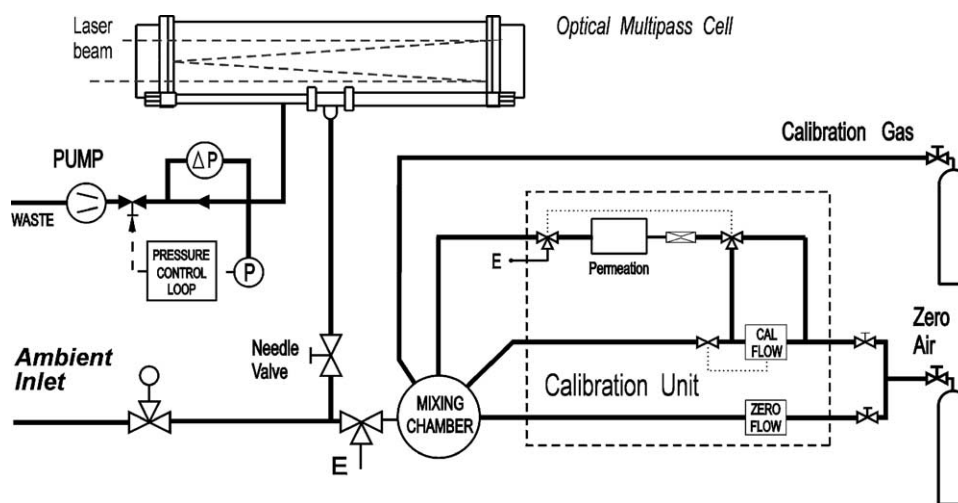


Fig. 8. Integration of the calibration system into a TDLS system. The pressure is typically below 100 mbar in the optical multipass cell and kept constant by an active pressure control loop. Besides the permeation based calibration gases, industrial gas mixtures from steel cylinders or lecture bottles can be added.

15; this is due to drift effects of the background structure, as also confirmed by Allan variance tests. In the following discussion the relevant precision parameters are evaluated using 10 values for each concentration level. Therefore, for future measurements with an identical system this measurement cycle is mandatory when specifying precision parameters. The LDL was found to be 325 pptv and the repeatability changes from 0.565 to 1.07 ppbv, depending on the number of samples taken. As a next step a calibration experiment in the range 20–260 ppbv  $\text{NO}_2$  has been performed, using a pressurized gas mixture of 260 ppbv  $\text{NO}_2$  ( $\pm 5\%$ ) in synthetic air as the test sample and different dilution flows of nitrogen were provided by a calibrated flow controller (Fig. 9c). The instrument was calibrated with a concentration of 20 ppbv  $\text{NO}_2$ , provided by the calibration system shown in Figs. 7 and 8. Since the high concentration values are extrapolated from the calibration signal, the reproducibility at 250 ppbv  $\text{NO}_2$  is about 1 ppbv. The measured values and the calculated linear regression lines are shown in Fig. 9d. A linear behavior is expected for an absorption below 1% in terms of optical density, which corresponds in our set-up to  $\sim 150$  ppbv  $\text{NO}_2$ . At higher absorption levels the non-linearity of the exponential function in the Lambert–Beer-law has to be considered (e.g. at 260 ppbv the relative error is 0.75%). From Fig. 9d it can be seen that the specified concentration level of 260 ppbv  $\pm 5\%$  (manufactured by a 100 times dilution of

an original calibration mixture, which has been measured by a chemiluminescence instrument) could not be verified, because the slope from the linear regression analysis indicates a value of 242 ppbv  $\text{NO}_2 \pm 0.4\%$ , i.e. 7% smaller or 2% outside the specified range.

For performance tests of a formaldehyde sensor  $\text{H}_2\text{CO}$  an “aqueous solution” has been used as a permeation source. Wafers are commercially available for many molecules; they have the advantage that calibration of these devices is traceable to the mass loss, which can be determined from periodic weighings as shown for  $\text{NO}_2$  in Fig. 6, and the dilution flow determined by calibrated mass flow controller. This is true when the wafer contains only one substance. In contrast, the “aqueous solution” device consists of a bottle containing a solution of the target substance with a polyethylene tubing submerged in the solution. The target substance then permeates from the solution outside into the tubing and is flushed out by the carrier gas. These solution permeation devices have to be calibrated by other measurement techniques, because the weight loss cannot be attributed to the target substance. In our system we used a solution permeation device for  $\text{H}_2\text{CO}$ , calibrated by an enzymatic-fluorometric method [113] – We also checked a direct absorption measurement at  $3.5 \mu\text{m}$  where line parameters are known. Alternatively wafers with paraformaldehyde are available for  $\text{H}_2\text{CO}$ , but they require a temperature of  $80^\circ\text{C}$ , which cannot

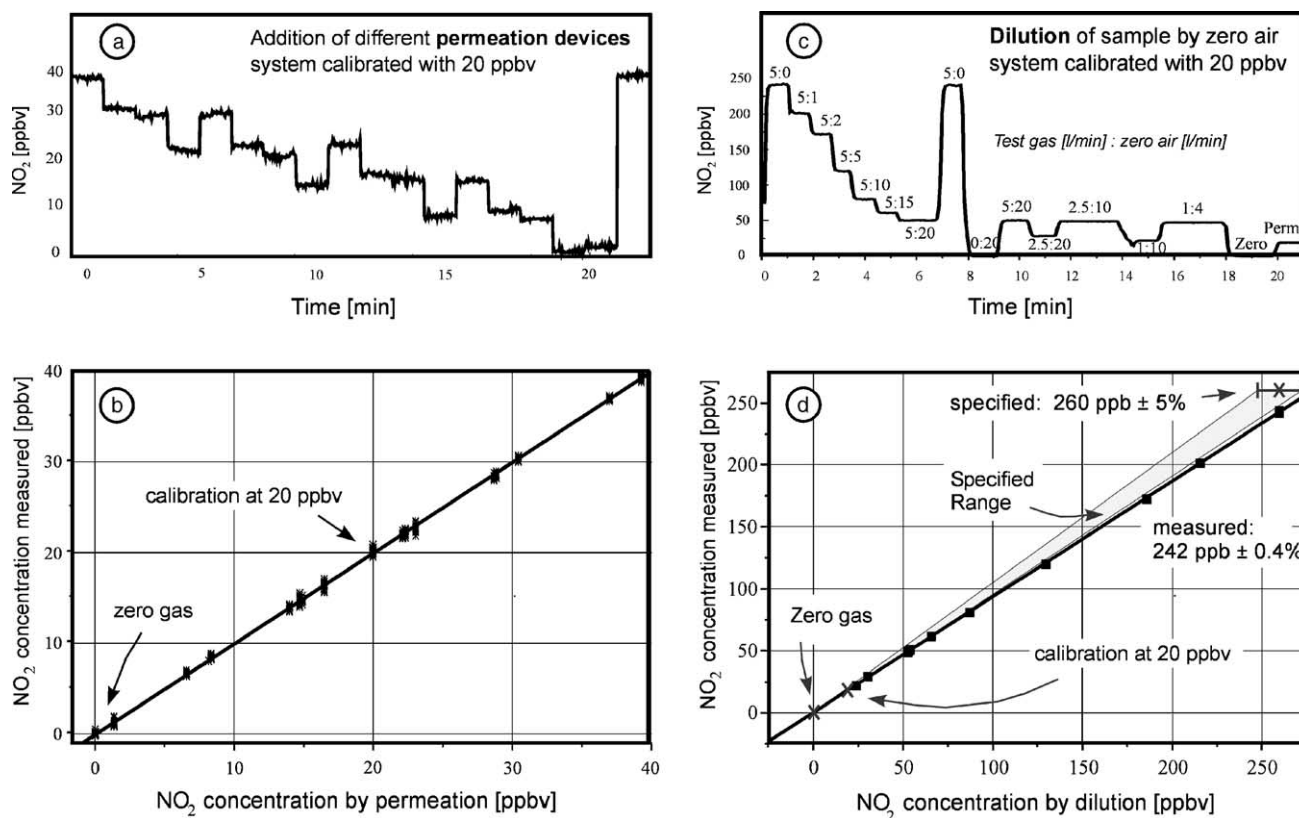


Fig. 9. (a) Example of a TDLS calibration by adding different concentrations from  $\text{NO}_2$  permeation devices from cascaded ovens and the (b) corresponding calibration function. (c) As an alternative, pressurized industrial calibration gases from steel cylinders can be diluted to (d) record a calibration function.

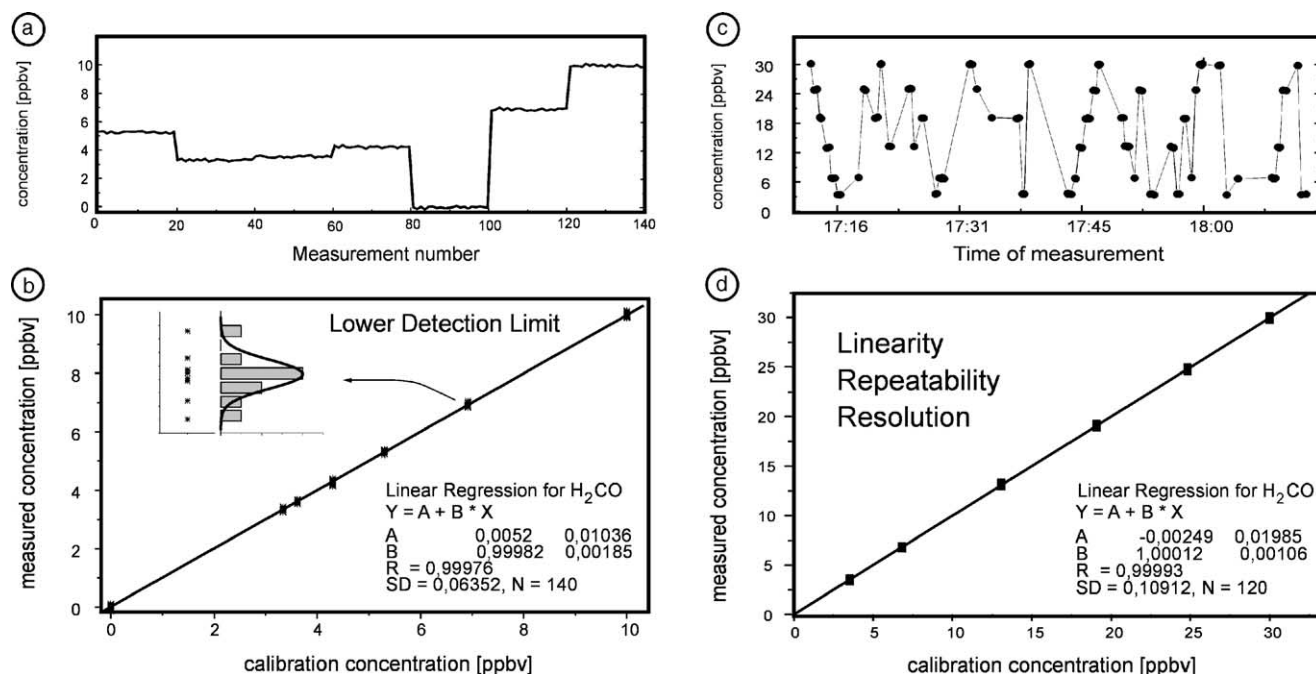


Fig. 10. (a) A variable dilution flow from a formaldehyde calibration source has been used to record a (b) linear calibration function for H<sub>2</sub>CO measurements by subsequent measurements of 20 values for each sample. (c) In an other experiment the sequence was changed to rapid changes in the concentration levels and again a (d) linear calibration function has been recorded.

be provided by our oven system. The calibration function for H<sub>2</sub>CO measurements was determined using only one permeation device, and different concentration levels were prepared by a changing the dilution flow. The calibration signal was adjusted to 10 ppbv at a dilution flow of 4.51 l min<sup>-1</sup> (FC E: 3.98 l min<sup>-1</sup> and FC A: 0.53 l min<sup>-1</sup>). There were 20 measurement values for each concentration level with calibration and background measurements before each group (Fig. 10a). During the analysis no outliers have been found, and the hypothesis of linearity is accepted. The LDL was determined as 110 pptv and the repeatability as 186 pptv. Finally, a calibration function has been recorded using an additional flow controller which dumps out a part of the calibration gas flow before entering the mixing chamber. When we reduced the delay times after switching valves in the system, the different calibration levels could be reached faster, which resulted in a linear calibration function, shown in Fig. 10c and d. During the analysis no outliers have been found and the hypothesis of linearity was accepted. The LDL was 188 pptv and the repeatability 298 pptv.

## 5. Summary and conclusions

Tunable diode-laser spectroscopy is a powerful tool for analytical applications where high sensitivity, detection speed and the possibility of highly specific and simultaneous in situ measurements of atmospheric trace gases is required. While many improvements in modern TDLS system development focus on optimizing electronics and

optical components, much less effort has been put into post detection signal processing and adaptive control. It was the purpose of this paper to discuss post-detection signal processing strategies for tunable diode-laser spectroscopy. Spectroscopic signals may vary in frequency due to fluctuations or transients in the laser current and in amplitude due to changing background structures such as moving fringes. Broad fringes can appear as a linear slope superimposed on the desired TDLAS signal. The conventionally used linear regression scheme may report wrong concentration data when the signal is distorted, which is especially critical at low ambient concentrations. Depending on the direction of the slope of the background the linear regression tends to over- or underestimate the concentration of the ambient gas. Much more critical is the impact of drifts of ambient spectra relative to the calibration spectrum. These drift effects can lead to a significant underestimation of concentration values. A spectrometer with critical drifts can provide extremely low concentration values which result from the drift effects rather than from changes in ambient trace gas concentrations. To address these problems, an online shift or software correction improves the confidence range of the data significantly. To reduce the sensitivity towards changes in the background structure, the multiple linear regression has been found to be useful, because it allows one to account for linear, quadratic and even higher order residual structures due to changes in the background signal. The sensitivity of an TDLS instrument can be improved by averaging over a long time scale, but at optical densities of the order of 10<sup>-6</sup> the sensitivity is usually limited by fringes

due to unwanted étalons. In principle, this limitation can be avoided by subtracting the background (zero air) absorption spectra from the spectrum of ambient air. This procedure inherently assumes that the instrument is stable during the time needed for the acquisition of both spectra, i.e. that the fringes do not move in the meantime. The stability and the resulting detection limits of the instrument can conveniently be described by the Allan variance. The Allan plot provides information about the optimum averaging time for the spectra and so allows the prediction of the ultimate detection limits of the spectrometer. If the optimum integration time has already been determined for a instrument, it may be necessary to check its value for time to time, especially under field operating conditions or in monitoring stations system where parameters could change and so degrade the system performance. An automated spectrometer can run the stability tests under computer control by analyzing a time series of low level calibration data. The system can then adopt automatically the newly determined averaging time constant to collect background and ambient spectra.

System audits and intercomparisons of system performance require internationally accepted definitions of the figures of merit characterizing the instrument. Many differences found in the literature arise from different definitions of the terms such as sensitivity, detection limit, determination limit, accuracy, and precision. The performance of the system has to be routinely checked using calibration gases of varying concentrations and a zero gas. The best zero gas is the air sample from which the target compound was taken out by some sort of a scrubber. Such zero gas can account for spectral interferences by other trace compounds in the air. If this is not possible, synthetic air or pure nitrogen can be used. Calibration gases are usually procured as premixed gas mixtures in high pressure passivated cylinders of a known, certified concentration. For linearity tests these gases are diluted to the desired concentration or used directly without dilution. This method is suitable for most unpolar and some slightly polar compounds such as methane, carbon monoxide, nitrous oxide, most of the hydrocarbons and halocarbons. Since polar compounds are usually adsorbed by the walls of the high pressure cylinders, their concentrations would be too unstable for calibration purposes. Calibration mixtures of polar compounds such as nitric acid, ammonia, aldehydes, alcohols, organic acids, are usually generated by permeation or other diffusion devices and the concentrations are adjusted by the flow of the carrier gas or by additional dilution stages. The certified concentration of calibration mixtures in high pressure cylinders is usually traceable to gravimetric procedures. The permeation rate of the permeation devices is also determined gravimetrically as well.

For quality assurance the application of the ISO regulation for the determination of performance characteristics of measurement methods has been discussed in the context of TDLS. A calibration scheme for TDLS instruments has been presented which meets ISO requirements and allows multi-point and multi component calibration in an automated

operating environment designed for field applications. The linearity of TDLS measurements over a wide concentration range has been shown for NO<sub>2</sub> and formaldehyde. Terms like detection limit and repeatability have been used according with ISO standards and the lower detection limit has been derived from a calibration function.

## References

- [1] C.R. Webster, R.T. Menzies, E.D. Hinkley, *Infrared Laser Absorption: Theory and Applications*, in: R.M. Measures (Ed.), *Laser Remote Chemical Analysis - Chemical Analysis Series Vol. 94*, John Wiley & Sons, New York (1988) 163–532.
- [2] H.I. Schiff, G.I. Mackay, J. Bechara, in: M.W. Sigrist (Ed.), *Air Monitoring by Spectroscopic Techniques*, Chemical Analysis Series, vol. 127, Wiley, New York, 1994.
- [3] D.J. Brassington, in: R.E. Hester, R.J. Clark (Eds.), *Spectroscopy in Environmental Science, Advances in Spectroscopy*, vol. 24, Wiley, Chichester, 1994, pp. 85–148.
- [4] W. Mankin, E. Atlas, C. Cantrell, F. Eisele, A. Fried, in: G.P. Brasseur, J. Orlando, G.S. Tyndall (Eds.), *Atmospheric Chemistry and Global Change*, Oxford Press, New York, Oxford, 1999, p. 654.
- [5] R.F. Curl, F.K. Tittel, *Tunable infrared laser spectroscopy*, *Ann. Rep. Prog. Chem. C* 98 (2002) 217–270.
- [6] F.K. Tittel, D. Richter, A. Fried, in: I.T. Sorokina, K.L. Vodopyanov (Eds.), *Topics in Applied Physics*, Springer, Heidelberg, 2002.
- [7] M.S. Zahniser, D.D. Nelson, C.E. Kolb, in: K. Kohse-Höinghaus, J.B. Jeffries (Eds.), *Applied Combustion Diagnostics*, Taylor & Francis, New York, 2002, p. 648.
- [8] P. Werle, in: P. Hering, J.P. Lay, S. Stry (Eds.), *Lasers in Environmental and Life Sciences—Modern Analytical Methods*, Springer, Heidelberg, 2004, pp. 223–243.
- [9] P. Werle, *Spectrochim. Acta A* 54 (1998) 197–236.
- [10] P. Werle, K. Maurer, R. Kormann, R. Mücke, F. D'Amato, T. Lancia, A. Popov, *Spectrochim. Acta A* 58 (2002) 2361–2372.
- [11] J. Ye, L.S. Ma, J.L. Hall, *J. Opt. Soc. Am. B* 15 (1997) 6–14.
- [12] P. Werle, R. Mücke, F. D'Amato, T. Lancia, *Appl. Phys. B* 67 (1998) 307–315.
- [13] S.I. Chou, D.S. Baer, R.K. Hanson, *Appl. Opt.* 36 (1997) 3288–3292.
- [14] R.M. Mihalcea, M.E. Webber, D.S. Baer, R.K. Hanson, G.S. Feller, W.B. Chapman, *Appl. Phys. B* 67 (1998) 288.
- [15] G. Durry, G. Megie, *Appl. Opt.* 38 (1999) 7342.
- [16] L. Gianfrani, P. De Natale, G. De Natale, *Appl. Phys. B* 70 (2000) 467.
- [17] G. Durry, G. Megie, *Appl. Opt.* 39 (2000) 5801.
- [18] R. Chauv, B. Lavorel, *Appl. Phys. B* 72 (2001) 237–240.
- [19] G. Gagliardi, R. Restieri, G. De Biasio, P. De Natale, F. Cotrufo, L. Gianfrani, *Rev. Sci. Instrum.* 72 (2001) 4228.
- [20] M.E. Webber, R. Claps, F.V. English, F.K. Tittel, J.B. Jeffries, R.K. Hanson, *Appl. Opt.* 40 (2001) 4395–4403.
- [21] P. de Natale, L. Gianfrani, G. de Natale, *J. Volcanol. Geotherm. Res.* 109 (2001) 235–245.
- [22] E.C. Richard, K.K. Kelly, R.H. Winkler, R. Wilson, T.L. Thompson, R.J. McLaughlin, A.L. Schmeltekopf, A.F. Tuck, *Appl. Phys. B* 75 (2002) 183–194.
- [23] G. Durry, A. Hauchecorne, J. Ovarlez, H. Ovarlez, I. Pouchet, V. Zeninari, B. Parvitte, *J. Atmos. Chem.* 43 (2002) 175–194.
- [24] F. D'Amato, P. Mazzinghi, F. Castagnoli, *Appl. Phys. B* 75 (2002) 195–202.
- [25] C. Claveau, M. Lepere, G. Dufour, A. Valentin, A. Henry, C. Camy-Peyret, D. Hurtmans, *Spectrochim. Acta A* 58 (2002) 2313–2321.

- [26] A.G. Berezin, O.V. Ershov, A.I. Nadezhdinskii, *Appl. Phys. B* 75 (2002) 203–214.
- [27] R.T. Wainner, B.D. Green, M.G. Allen, M.A. White, J. Stafford-Evans, R. Naper, *Appl. Phys. B* 75 (2002) 249–254.
- [28] P. Werle, F. Slemr, K. Maurer, R. Kormann, R. Mücke, B. Jänker, *Opt. Lasers Eng.* 37 (2002) 101–114.
- [29] E.R.T. Kerstel, G. Gagliardi, L. Gianfrani, H.A.J. Meijer, R. van Trigt, R. Ramaker, *Spectrochim. Acta A* 58 (2002) 2389–2396.
- [30] H. Teichert, T. Fernholz, V. Ebert, *Appl. Opt.* 42 (2003) 2043–2051.
- [31] J.C. Nicolas, A.N. Baranov, Y. Cuminal, Y. Roillard, J.C. Alibert, *Appl. Opt.* 37 (1998) 7906–7911.
- [32] P. Werle, A. Popov, *Appl. Opt.* 38 (1999) 1494–1501.
- [33] A. Vicet, D.A. Yarekha, A. Pérona, Y. Rouillard, S. Gaillard, A.N. Baranov, *Spectrochim. Acta A* 58 (2002) 2405–2412.
- [34] R.D. May, C.R. Webster, *J. Geophys. Res.* 94 (1989) 16343–16350.
- [35] D.S. Bomse, A.C. Stanton, J.A. Silver, *Appl. Opt.* 31 (1992) 718–731.
- [36] H.I. Schiff, D.R. Karecki, G.W. Harris, D.R. Hastie, G.I. Mackay, *J. Geophys. Res.* 95 (1990) 10147–10153.
- [37] G.W. Sachse, G.F. Hill, L.O. Wade, M.G. Perry, *J. Geophys. Res.* 92 (1987) 2071–2081.
- [38] A. Fried, J.R. Drummond, B. Henry, J. Fox, *Appl. Opt.* 30 (1991) 1916–1932.
- [39] P. Werle, F. Slemr, M. Gehrtz, C. Bräuchle, *Appl. Phys. B* 49 (1989) 99–108.
- [40] M. Tacke, *Infrared Phys. Technol.* 36 (1995) 447–463.
- [41] M.S. Zahniser, D.D. Nelson, J.B. McManus, P.L. Kebabian, *Philos. Trans. R. Soc. Lond.* 351 (1995) 371–379.
- [42] A. Fried, S. Sewell, B. Henry, B. Wert, T. Gilpin, J.R. Drummond, *J. Geophys. Res.* 102 (1997) 6253–6266.
- [43] T. Güllük, H.E. Wagner, F. Slemr, *Rev. Sci. Instrum.* 68 (1997) 230.
- [44] A. Fried, B. Henry, B. Wert, S. Sewell, J.R. Drummond, *Appl. Phys. B* 67 (1998) 317.
- [45] D.D. Nelson, M.S. Zahniser, J.B. McManus, C.E. Kolb, J.L. Jimenez, *Appl. Phys. B* 67 (1998) 433–441.
- [46] F.G. Wienhold, H. Fischer, P. Hoor, V. Wagner, R. Königstedt, G.W. Harris, J. Anders, R. Grisar, M. Knothe, W.J. Riedel, F.J. Lübken, T. Schilling, *Appl. Phys. B* 67 (1998) 411.
- [47] A. Nadezhdinskii, S. Berezin, S. Chernin, O. Ershov, V. Kutnyak, *Spectrochim. Acta A* 55 (1999) 2083–2089.
- [48] D.C. Scott, R.L. Herman, C.R. Webster, R.D. May, G.J. Flesch, E.J. Moyer, *Appl. Opt.* 38 (1999) 4809.
- [49] J. Röpcke, L. Mechold, M. Käning, J. Anders, F.G. Wienhold, D. Nelson, M. Zahniser, *Rev. Sci. Instrum.* 71 (2000) 3706.
- [50] R. Kormann, H. Müller, P. Werle, *Atmos. Environ.* 35 (2001) 2533–2544.
- [51] P. Werle, R. Kormann, *Appl. Opt.* 40 (2001) 846.
- [52] G. Toci, P. Mazzinghi, B. Mielke, L. Stefanutti, *Opt. Lasers Eng.* 37 (2002) 459–480.
- [53] M. Loewenstein, H. Jost, J. Grose, J. Eilers, D. Lynch, S. Jensen, J. Marmie, *Spectrochim. Acta A* 58 (2002) 2329–2345.
- [54] J.B. McManus, M.S. Zahniser, D.D. Nelson, L.R. Williams, C.E. Kolb, *Spectrochim. Acta: Part A* 58 (2002) 2465–2479.
- [55] C. Roller, K. Namjou, J. Jeffers, W. Potter, P.J. McCann, J. Grego, *Opt. Lett.* 27 (2002) 107–109.
- [56] M. Lepère, A. Valentin, A. Henry, C. Camy-Peyret, G. Blanquet, J.C. Populaire, A.W. Mantz, *Spectrochim. Acta A* 58 (2002) 2413–2419.
- [57] R. Kormann, H. Fischer, C. Gurk, F. Helleis, T. Klüpfel, K. Kowalski, R. Königstedt, U. Parchatka, V. Wagner, *Spectrochim. Acta A* 58 (2002) 2489–2498.
- [58] D. Richter, M. Erdelyi, R.F. Curl, F.K. Tittel, C. Oppenheimer, H.J. Duffell, M. Burton, *Opt. Lasers Eng.* 37 (2002) 171–186.
- [59] J. Faist, F. Capasso, D.L. Sivco, C. Sirtori, A.L. Hutchinson, A.Y. Cho, *Science* 264 (1994) 553–555.
- [60] C. Sirtori, P. Kruck, S. Barbieri, P. Collot, J. Nagle, M. Beck, J. Faist, U. Oesterle, *Appl. Phys. Lett.* 73 (1998) 3486.
- [61] K. Namjou, S. Cai, E.A. Whittaker, J. Faist, C. Gmachl, F. Capasso, D.L. Sivco, A.Y. Cho, *Opt. Lett.* 23 (1998) 219–221.
- [62] S.W. Sharpe, J.F. Kelly, J.S. Hartman, C. Gmachl, F. Capasso, D.L. Sivco, J.N. Baillargeon, A.Y. Cho, *Opt. Lett.* 23 (1998) 1397–1398.
- [63] R.M. Williams, J.F. Kelly, J.S. Hartmann, S.W. Sharpe, M.S. Taubmann, J.L. Hall, F. Capasso, C. Gmachl, D.L. Sivco, J.N. Baillargeon, A.L. Hutchinson, A.Y. Cho, *Opt. Lett.* 24 (1999) 1844–1846.
- [64] A.A. Kosterev, R.F. Curl, F.K. Tittel, C. Gmachl, F. Capasso, D.L. Sivco, J.N. Baillargeon, A.L. Hutchinson, A.Y. Cho, *Opt. Lett.* 24 (1999) 1762–1764.
- [65] A.A. Kosterev, F.K. Tittel, C. Gmachl, F. Capasso, D.L. Sivco, J.N. Baillargeon, A.L. Hutchinson, A.Y. Cho, *Appl. Opt.* 39 (2000) 6866.
- [66] A.A. Kosterev, F.K. Tittel, R.F. Curl, M. Rochat, J. Faist, *Appl. Phys. B* 75 (2002) 351–357.
- [67] L. Hvozdar, S. Gianordoli, G. Strasser, W. Schrenk, K. Unterrainer, E. Gornik, C. Murthy, M. Kraft, V. Pustogov, B. Mizaikoff, *Physica E* 7 (2000) 37–39.
- [68] W. Schrenk, N. Finger, S. Gianordoli, L. Hvozdar, G. Strasser, E. Gornik, *Appl. Phys. Lett.* 76 (2000) 253–255.
- [69] M. Beck, D. Hofstetter, T. Aellen, J. Faist, U. Oesterle, M. Ilegems, E. Gini, H. Melchior, *Science* 295 (2002) 301–305.
- [70] A.A. Kosterev, F.K. Tittel, *Chemical sensors based on quantum cascade lasers*, *IEEE J. Quant. Elect.* 38 (2002) 582–591.
- [71] C.R. Webster, G.J. Flesh, D.C. Scott, J.E. Swanson, R.D. May, W.S. Woodward, C. Gmachl, F. Capasso, D.L. Sivco, J.N. Baillargeon, A.L. Hutchinson, A.Y. Cho, *Appl. Opt.* 40 (2001) 321.
- [72] D.D. Nelson, J.H. Shorter, J.B. McManus, M.S. Zahniser, *Appl. Phys. B* 75 (2002) 343–350.
- [73] L.S. Rothman, R.R. Gamache, R.H. Tipping, C.P. Rinsland, M.A.H. Smith, D.C. Brenner, V. Malathy Devi, J.M. Flaud, C. Camy-Peyret, A. Perrin, A. Goldman, S.T. Massie, L.R. Brown, R.A. Toth, *J. Quant. Spectrosc. Radiat. Transfer* 48 (1992) 469–507.
- [74] J.U. White, *J. Opt. Soc. Am.* 66 (1976) 411–416.
- [75] D.R. Herriott, H.J. Schulte, *Appl. Opt.* 4 (1965) 883–889.
- [76] S.M. Chernin, *J. Mod. Opt.* 39 (1992) 525.
- [77] J.B. McManus, P.L. Kebabian, M.S. Zahniser, *Appl. Opt.* 34 (1995) 3336–3348.
- [78] F. D’Amato, M. de Rosa, *Opt. Lasers Eng.* 37 (2002) 533–551.
- [79] K. Uehara, *Opt. Lett.* 12 (1987) 81–83.
- [80] P. Laguna, R. Jane, E. Masgrau, P. Caminal, *Signal Process.* 48 (1996) 193–203.
- [81] P. Werle, B. Scheumann, J. Schandl, *Opt. Eng.* 33 (1994) 3093–3105.
- [82] H. Riris, C.B. Carlisle, R.E. Warren, D.E. Cooper, *Opt. Lett.* 19 (1994) 144–148.
- [83] H. Riris, C.B. Carlisle, R.E. Warren, *Appl. Opt.* 33 (1994) 5506–5511.
- [84] D.P. Leleux, R. Claps, W. Chen, F.K. Tittel, T.L. Harman, *Appl. Phys. B* 74 (2002) 85–93.
- [85] R.S. Disselkamp, J.F. Kelly, R.L. Sams, G.A. Anderson, *Appl. Phys. B* 75 (2002) 359–366.
- [86] P. Werle, R. Mücke, F. Slemr, *Appl. Phys. B* 57 (1993) 131–139.
- [87] F.C. Fehsenfeld, J.W. Drummond, U.K. Roychowdhury, P.J. Galvin, E.J. Williams, M.P. Buhr, D.D. Parrish, G. Hübler, A.O. Langford, J.G. Calvert, B.A. Ridley, F. Grahek, B.G. Heikes, G.L. Kok, J.D. Shetter, J.G. Walega, C.M. Elsworth, R.B. Norton, D.W. Fahey, P.C. Murphy, C. Hovermale, V.A. Mohnen, K.L. Demerjian, G.I. Mackay, H.I. Schiff, *J. Geophys. Res.* 95 (1990) 3579–3597.
- [88] G.L. Gregory, J.M. Hoell Jr., M.A. Carroll, B.A. Ridley, D.D. Davis, J. Bradshaw, M.O. Rodgers, S.T. Sandholm, H.I. Schiff, D.R. Hastie, D.R. Karecki, G.I. Mackay, G.W. Harris, A.L. Torres, A. Fried, *J. Geophys. Res.* 95 (1990) 10103–10127.

- [89] A. Fried, L. Nunnermacker, B. Cadoff, R. Sams, N. Yates, W. Dorko, R. Dickerson, E. Winstead, *J. Geophys. Res.* 95 (1990) 10139–10146.
- [90] D.D. Parrish, F.C. Fehsenfeld, *Atmos. Environ.* 34 (2000) 1921–1957.
- [91] ISO 9169, Air Quality—Determination of Performance Characteristics of Measurement Methods, DIN Deutsches Institut für Normung e.V., Beuth Verlag GmbH, Berlin, 1996.
- [92] VDI 2449/1: Measurement Methods Test criteria—Determination of Performance Characteristics for the Measurement of Gaseous Pollutants (Immision), DIN Deutsches Institut für Normung e.V., Beuth Verlag GmbH, Berlin, 1995.
- [93] VDI 2449/2: Basic Concepts for Characterization of a Complete Procedure—Glossary of Terms, DIN Deutsches Institut für Normung e.V., Beuth Verlag GmbH, Berlin, 1987.
- [94] VDI 2449/3: Measurement Methods Test criteria—General Method for the Determination of the Uncertainty of Calibrate Measurement Methods, DIN Deutsches Institut für Normung e.V., Beuth Verlag GmbH, Berlin, 2001.
- [95] ISO 5725, Accuracy (Trueness and Precision) of Measurement Methods and Results—Basic Method for the Determination of Repeatability and Reproducibility of a Standard Measurement Method, DIN Deutsches Institut für Normung e.V., Beuth Verlag GmbH, Berlin, 2002.
- [96] L. Sachs, *Angewandte Statistik*, Springer, Berlin, 1978.
- [97] J.K. Taylor, *Quality Assurance of Chemical Measurements*, Lewis, Chelsea, 1988.
- [98] F.E. Grubbs, *G. Beck, Technometrics* 14 (1972) 847–854.
- [99] Analytical Methods Committee, *Analyst* 113 (1988) 1469–1471.
- [100] J.N. Miller, *Basic statistical methods for analytical chemistry*, *Analyst* 116 (1991) 3–14.
- [101] VDI 2100/4, Gaseous Ambient Air Measurement, Indoor Air Pollution Measurements, Gas Chromatic Determination of Organic Compounds, Calibration Procedures as a Measure for Quality Assurance, DIN Deutsches Institut für Normung e.V., Beuth Verlag GmbH, Berlin, 2003.
- [102] R.S. Barratt, *Analyst* 106 (1981) 817–849.
- [103] A.E. O’Keefe, G.C. Ortman, *Anal. Chem.* 38 (1966) 760–763.
- [104] N. Beltz, W. Jaeschke, F.X. Meixner, *Thermochim. Acta* 103 (1986) 57–62.
- [105] G.O. Nelson, *Gas Mixtures: Preparation and Control*, Lewis Publishers, 1992.
- [106] A.T. Mohammadi, T. Matsuura, S. Sourirajan, *J. Membr. Sci.* 98 (1995) 281–286.
- [107] T.J. Bruno, *J. Chromatogr. A* 704 (1995) 157–162.
- [108] P.H. Huang, *Sens. Actuators B* 53 (1998) 125–127.
- [109] K.R. Lassey, C.F. Walker, A.M.S. McMillan, M.J. Ulyatt, *Chemosphere* 3 (2001) 367–376.
- [110] A. Fried, B. Henry, S. Sewell, *J. Geophys. Res.* 103 (1998) 18,895–18,906.
- [111] P.D. Goldan, W.C. Kuster, D.L. Albritton, *Atmos. Environ.* 20 (1986) 1203–1208.
- [112] A. Fried, Y.-N. Lee, G. Frost, B. Wert, B. Henry, D.R. Drummond, G. Hübler, T. Jobson, *J. Geophys. Res.* 107 D13 (2002), pp. 10.1029/2000JD000260.
- [113] A.L. Lazrus, K.L. Fong, J.A. Lind, *Anal. Chem.* 60 (1980) 1074–1078.